In vivo Dissection of Long Range Inputs to the Rat Barrel Cortex

by Wanying Zhang

Submitted in partial fulfillment of the requirements for the degree of Doctor of Philosophy under the Executive Committee of the Graduate School of Arts and Sciences

Columbia University
2014

ABSTRACT

IN VIVO DISSECTION OF THE LONG RANGE INPUTS TO THE RAT BARREL CORTEX

WANYING ZHANG

Layer 1 (L1) of the cerebral cortex is a largely acellular layer that consists mainly of long-range projection axons and apical dendrites of deeper pyramidal neurons. In the rodent barrel cortex, L1 contains axons from both higher motor and sensory areas of the brain. Despite the abundance of synapses in L1 their actual contribution to sensory processing remains unknown. We investigated the impact of activating long-range axons on barrel cortex L2/3 pyramidal neurons in vivo using a combination of optogenetics and eletrophysiological techniques. The reason we target our investigation on L2/3 is because of its well-known sparse sensory responses. We hypothesize that long-range top-down inputs via L1 can provide the additional inputs necessary to unleash L2/3 and strongly influence sensory processing in S1. We focused on three main sources of BC-projecting synapses: the posterior medial nucleus of the thalamus (POm, the secondary somatosensory nucleus), the primary motor cortex (M1), and the secondary somatosensory cortex (S2).

Here we report that while activation of POm axons elicits strong EPSPs in most recorded L2/3 cells, activation of M1 or S2 axons elicited small or no detectable responses. Only POm activation boosted sensory responses in L2/3 pyramidal neurons. We also found that during wakefulness and under sedation, POM activation not only elicited a strong fast-onset EPSP in L2/3 neurons, but also a delayed persistent response. Pharmacological inactivation of POM abolished this persistent response but not the initial synaptic volley to L2/3. We conclude that the persistent response requires intrathalamic or thalamocortical circuits and cannot be mediated by

specialized synaptic terminals or intracortical circuitry.

Overall, our study suggests that the higher order thalamic nucleus provides more powerful network effect on L2/3 sensory processing than higher order cortical feedback inputs. POm activation not only directly boosts L2/3 sensory responses, but is also capable of influencing S1 signal processing for prolonged periods of time after stimulus onset and can potentially be important for other cognitive aspects of sensory computation.

Table of Contents

List of Figures

1.0 INTRODUCTION

During natural exploration, rats and mice use their facial whiskers to examine novel objects and environments. They sweep their whiskers back and forth to palpate the object of interest (a behavioral called whisking) to discern properties such as size, shape, and texture (Carvell and Simons 1990, Diamond, von Heimendahl et al. 2008, Hartmann 2011). Once the sensory perception of the object or environment is formed, the animal can make the proper behavioral responses (such as proceed with further investigate, prey-capture behavior, fight, flee, or ignore), and ensure its own survival. How the central nervous system transforms sensory inputs generated via seemingly simple exploratory behaviors into accurate representations of its environments is unknown and a topic of ongoing research.

The primary somatosensory cortex (S1) is required for the formation of sensory perception. Inactivation of the whisker area of S1 (also known as the barrel cortex) renders the animal unable to perform the simplest tactile detection tasks (Miyashita and Feldman 2013, Sachidhanandam, Sreenivasan et al. 2013). However, S1 does not function as an isolated unit but is instead reciprocally connected with several higher order cortical and subcortical areas. These areas are active during normal behavioral conditions, therefore their inputs to S1 should be considered as integral parts of the sensory-processing circuitry. Whereas the basic pathways for how sensory inputs ascend from the peripheral sensory organ (the whiskers) to S1 have been fairly well studied, how higher order top-down inputs influence S1 sensory processing is not well understood.

In this thesis we focus on the influences of three higher order brain areas on layer (L) 2/3 of S1. We compare the effects of inputs from the primary motor cortex (M1), and the posterior medial thalamic nucleus (POm), or the secondary somatosensory thalamic

nuclei and the secondary somatosensory cortex (S2) on L2/3 sensory processing. The first part of this introduction will focus on the basic circuitry underlying the rodent vibrissal sensory system as well as cortical sensory processing within S1, with a focus on the functional role of L2/3. The second part will introduce the three high-order brain regions and their connections with the whisker sensory system to provide an adequate overview on how top-down inputs are organized within the rodent somatosensory system.

1.1 ORGANIZATION OF THE RODENT WHISKER-BARREL SOMATOSENSORY SYSTEM

The rodent whisker-barrel system is comprised of two parallel pathways. In both, sensory information is generated by peripheral sensory neurons innervating the whisker pad. This information ascends through the brainstem, then the thalamus, and finally arrives at the cortex (**Fig 1.1**). Basic sensory processing is thought to occur in the direction of information flow: from periphery to S1. However, the circuitry is complicated by extensive cortical feedback to both the thalamic and brainstem nuclei. Cortical feedback connections result in the formation of several direct and indirect loops between different stages of sensory processing. The field has made great strides in elucidating how each of the stages in the whisker-barrel system processes sensory inputs individually, but still lacks global understanding of how the system behaves as a whole to create coherent representations of the tactile sensory environment.

The Lemniscal Pathway

The lemniscal pathway is considered the primary somatosensory pathway in the rodent vibrissal system. The whisker follicles are directly innervated by primary afferent sensory neurons residing in the trigeminal ganglion. Sensory information generated at the trigeminal ganglion is then sent to the nucleus principalis (PrV) of the brainstem trigeminal complex. The signal then ascends from the brainstem to the ventro-posterior medial nucleus (VPM) of the thalamus. VPM then innervates S1 barrel cortex (**Fig 1.1**,

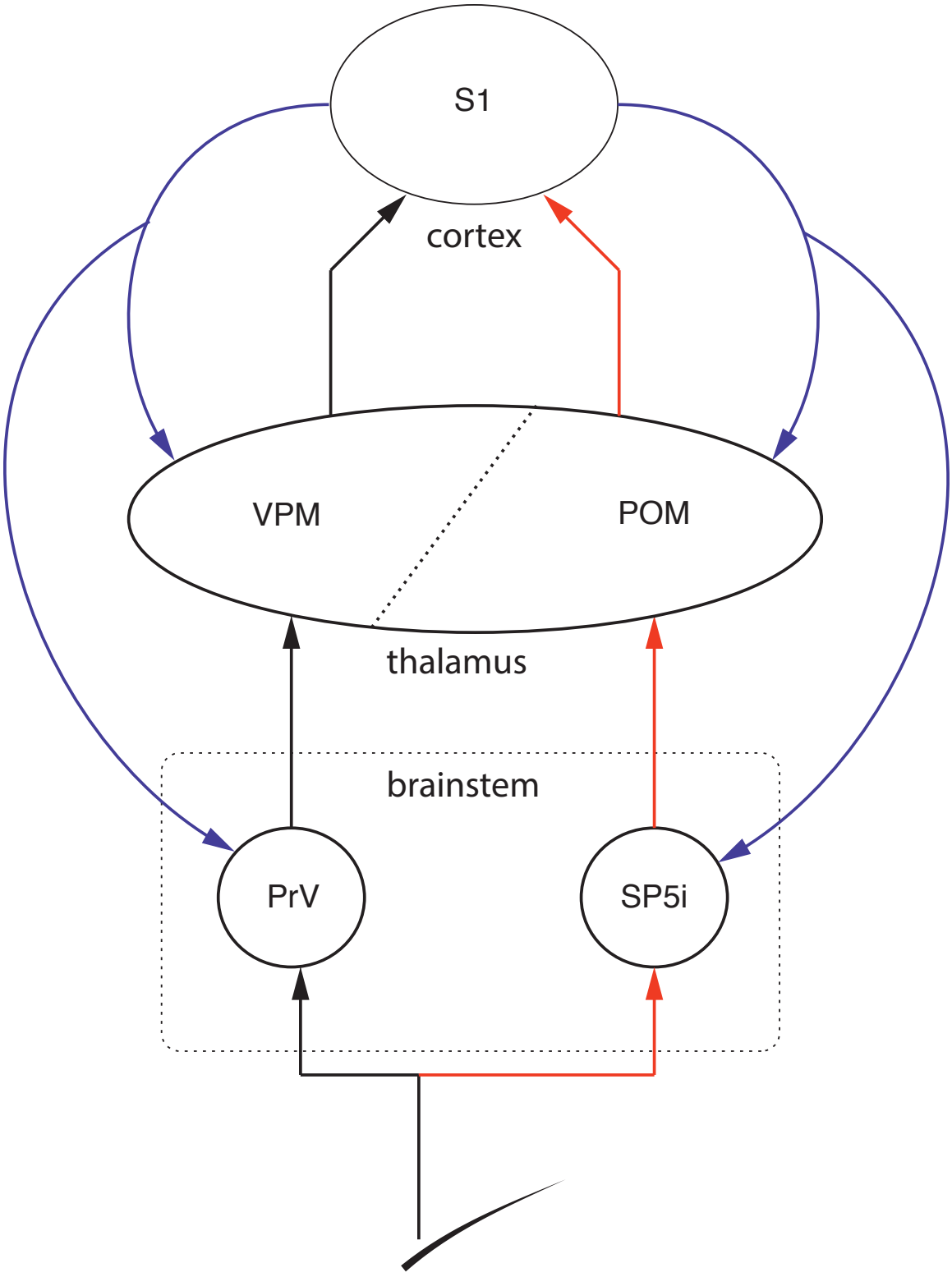

Fig 1.1 Major pathways of the whisker-barrel system. A simplified diagram illustrating the two parallel ascending pathways of the whisker-barrel sensory system (black, lemniscal pathway; red, paralemniscal pathway), as well as the cortical feedback inputs to subcortical areas (blue).

black lines). All stages of the lemniscal pathway maintain anatomically prominent topographical representation (barrels in S1, barreloids and barrelettes in VPM and PrV, respectively) of the whisker pad itself.

This strict topographical organization is also reflected in the functional properties of each unit of the lemniscal pathway. Every barreloid/barrelette/barrel responds robustly to deflections of a single whisker. This whisker is identified as the principal whisker (PW) of the unit. Neurons in the trigeminal ganglion respond robustly with short delays to PW stimulation, faithfully encoding specific stimulus properties such as direction, amplitude, and velocity (Zucker and Welker 1969, Lichtenstein, Carvell et al. 1990). The principal afferent neurons then converge onto PrV neurons in the brainstem. PrV neurons have larger receptive fields that include at least one adjacent whisker (AW) (Minnery and Simons 2002). Lesion studies in which ascending intersubnuclear axons were destroyed provided clear evidence that adjacent whisker responses in PrV rely primarily on projections from the spinal trigeminal complex to the PrV (Kwegyir-Afful, Bruno et al. 2005). Neurons in VPM inherit their response properties from the VPM-projecting PrV cells: strong, short-latency responses to PW and weaker responses to AWs (Chiaia, Rhoades et al. 1991, Diamond and Ebner 1992, Minnery and Simons 2002, Minnery, Bruno et al. 2003). Upon entering the cortex, the receptive fields of S1 neurons become drastically different from VPM neurons. L4 of S1, the main recipient layer of VPM inputs, shows much weaker responses to PW-stimulation. Cortical excitatory neurons optimally respond to high-velocity whisker stimulation, and are weakly directionally selective (Simons 1978, Carvell and Simons 1989, Bruno and Simons 2002).

There are several lines of top-down cortical feedback pathways within the lemniscal pathway. L6 of S1 contains corticothalamic neurons that form feedback modulatory connections onto distal dendrites of VPM neurons (Bourassa, Pinault et al. 1995, Killackey and Sherman 2003). These corticothalamic neurons have been shown to be almost completely silent *in vivo*, both spontaneously and in response to whisker stimulation (de Kock and Sakmann 2009, Constantinople and Bruno 2011). Under anesthesia, silencing the cortex does not affect the response properties of VPM neurons (Diamond and Ebner 1992). However, artificially activating L6 neurons can boost whisker responses in the aligned VPM barreloid. This suggests that when activated, L6 corticothalamic projections can affect sensory processing in the lemniscal pathway by selectively enhancing VPM sensory responses in certain barreloids over others (Temereanca and Simons 2004, Lee, Carvell et al. 2008). The circumstances under which these neurons can be high engaged are still unknown. S1 L5 corticofugal neurons are also known to innervate PrV neurons (Wise and Jones 1977). However, very little is known about the anatomical as well as physiological properties of these connections.

The Paralemniscal Pathway

The paralemniscal pathway is considered the secondary pathway for the rodent vibrissal system. Similar to the lemniscal pathway, sensory information also ascends through trigeminal ganglion → brainstem → thalamus → cortex in the paralemniscal pathway. In this case, the primary afferent sensory neurons innervate the spinal trigeminal subnucleus interpolaris (SP5i) of the brainstem instead of the PrV. Neurons in SP5i then innervate POm, and POm neurons send cortical projection axons to layers 1

and 5a of S1 (**Fig1.1**, red lines).

Unlike circuit elements within the lemniscal pathway, individual neurons in the paralemniscal pathway components do not encode whisker stimuli robustly or faithfully. SP5i neurons that project to POm have large receptive fields, and no prominent PW (Jaquin, Mooney et al. 1986, Furuta, Urbain et al. 2010). POm neurons, in spite of receiving substantial driving inputs from SP5i (Groh, Bokor et al. 2013), respond only weakly to whisker stimuli at long latencies (Diamond and Ebner 1992, Masri, Bezdudnaya et al. 2008, Masri, Quiton et al. 2009). Studies have suggested that POm neurons actually derive most, if not all, of their sensory responses from corticothalamic inputs from S1 (Diamond and Ebner 1992). Due to the large multi-whisker receptive fields of both SP5i and POm, these regions are only loosely topographically organized.

Both SP5i and POm receive substantial inputs from S1. Electrical stimulation of corticotrigeminal projecting neurons in barrel cortex can directly drive spiking of SP5i trigemino-thalamic projecting neurons with aligned and/or overlapping receptive fields (Furuta, Urbain et al. 2010). S1 L5 corticofugal neurons send collaterals to POm, which form large, glomeruli-like synapses onto POm neurons (Bourassa, Pinault et al. 1995). As mentioned previously, these strong corticothalamic projections are thought to drive the sensory responses of POm neurons. In addition to S1 cortical inputs, both SP5i and POm are highly susceptible to cholinergic modulation. Cholinergic axons from the pedunculopontine tegmental nucleus (PPT) form cholinergic (VAChT-positive) synapses directly onto SP5i dendrites and axons. Activation of these synapses by acetylcholine (ACh) agonists potentiates SP5i neuronal response to sensory stimuli (Timofeeva, Dufresne et al. 2005). POm also receives direct cholinergic input via the PPT and indirect

ACh-mediated modulation through zona incerta (ZI) (Masri, Trageser et al. 2006, Trageser, Burke et al. 2006). POm sensory responses are discussed in detail in section 1.3.1 below.

While we have extensive data on how neurons in each element of the lemniscal and paralemniscal pathways respond to passive whisker stimuli under anesthesia, how the rodent vibrissal sensory system functions as a whole during active sensing behavior remains elusive. The fact that cortical and neuromodulatory inputs can have deep impacts on sensory processing of both pathways suggests that instead of two simple parallel feed forward pathways for relaying sensory information, functions of these circuits and the dynamics of information flow within them are likely to be highly dynamic and dependent on the behavioral states of the animal. More studies need to be done in awake and behaving animals to elucidate the functional properties of these sensory pathways.

1.2 CIRCUITRY OF THE RODENT BARREL CORTEX

The rodent barrel cortex is so named for the discrete barrel-like cytoarchitectonic units in L4. Cortical columns within the barrel cortex are defined anatomically by the horizontal borders of each barrel. Neurons in each barrel-related column generally respond optimally to stimulation of a single topographically aligned facial PW. Processing of whisker-mediated sensory information is carried out by circuit interactions within and among the barrel columns.

Basic laminar organization and function of barrel cortex

Like all primary sensory cortices, the rodent S1 is thought to be comprised of six distinct cellular layers (**Fig 1.2**). As mentioned above, L4 has been thought of as the main thalamo-recipient layer. VPM cortical axons ramify in L4 and form dense clusters defines individual L4 barrels (Lu and Lin 1993, Wimmer, Bruno et al. 2010). L4 neurons innervate mostly other L4 neurons within the same barrel, as well as L2/3 neurons of the same column (Feldmeyer, Egger et al. 1999, Feldmeyer, Lubke et al. 2002, Lefort, Tomm et al. 2009). L2/3 projects to L2/3 and L5 neurons both within and outside of its home column, as well as to the supra- and infragranular cells of other cortical areas (Thomson and Bannister 1998, Feldmeyer, Lubke et al. 2006, Bruno, Hahn et al. 2009, Lefort, Tomm et al. 2009, Chen, Carta et al. 2013, Yamashita, Pala et al. 2013).

L5 can be roughly divided into two sub-layers: L5a and L5b. Both receive strong inputs from L2/3 of the same cortical column (Lubke and Feldmeyer 2007, Petreanu, Mao et al. 2009). Additionally, L5a is innervated by POm thalamocortical axons (Lu and

Lin 1993, Petreanu, Mao et al. 2009, Wimmer, Bruno et al. 2010, Ohno, Kuramoto et al. 2012); L5b neurons receive significant direct VPM inputs (White 1979, Oberlaender, de Kock et al. 2012, Constantinople and Bruno 2013). Neurons of both L5a and 5b then project a number of sub-cortical brain regions such as thalamus, the striatum, and the brainstem (Wise and Jones 1977, Killackey and Sherman 2003). L6 also receives direct VPM inputs as well as inputs from L4 of the same column (Oberlaender, de Kock et al. 2012, Constantinople and Bruno 2013). L6 contain conticothalamic-projecting neurons whose axons innervate either VPM or POm (Bourassa, Pinault et al. 1995). Lastly, L1 is a mostly acellular layer comprised of horizontal projection axons from higher order cortical and sub-cortical regions, as well as the apical dendrites of L2/3 and L5 pyramidal neurons (Lu and Lin 1993, Cauller, Clancy et al. 1998, Petreanu, Mao et al. 2009). In addition to the neuropil, L1 is also sparsely populated by a wide variety of local inhibitory neurons (Gabbott and Somogyi 1986). Interestingly, most L1 interneurons express ionotropic serotonin receptors (Lee, Hjerling-Leffler et al. 2010).

Functionally, L4, L5 and L6 neurons show the shortest subthreshold response latencies to passive PW stimulation, reflecting their reception of direct VPM input (Constantinople and Bruno 2013). L4 and L6 subthreshold sensory responses also show the strongest preference to PW stimulation, responding weakly to 1-2 AWs (Brecht and Sakmann 2002, de Kock, Bruno et al. 2007, Ramirez, Pnevmatikakis et al. 2014). L2/3 and L5 neurons have much larger subthreshold receptive fields, including most, if not all 8 AWs immediately surrounding the PW (Brecht, Roth et al. 2003, Manns, Sakmann et al. 2004, Ramirez, Pnevmatikakis et al. 2014).

Most previous studies on the receptive field properties of S1 neurons have been

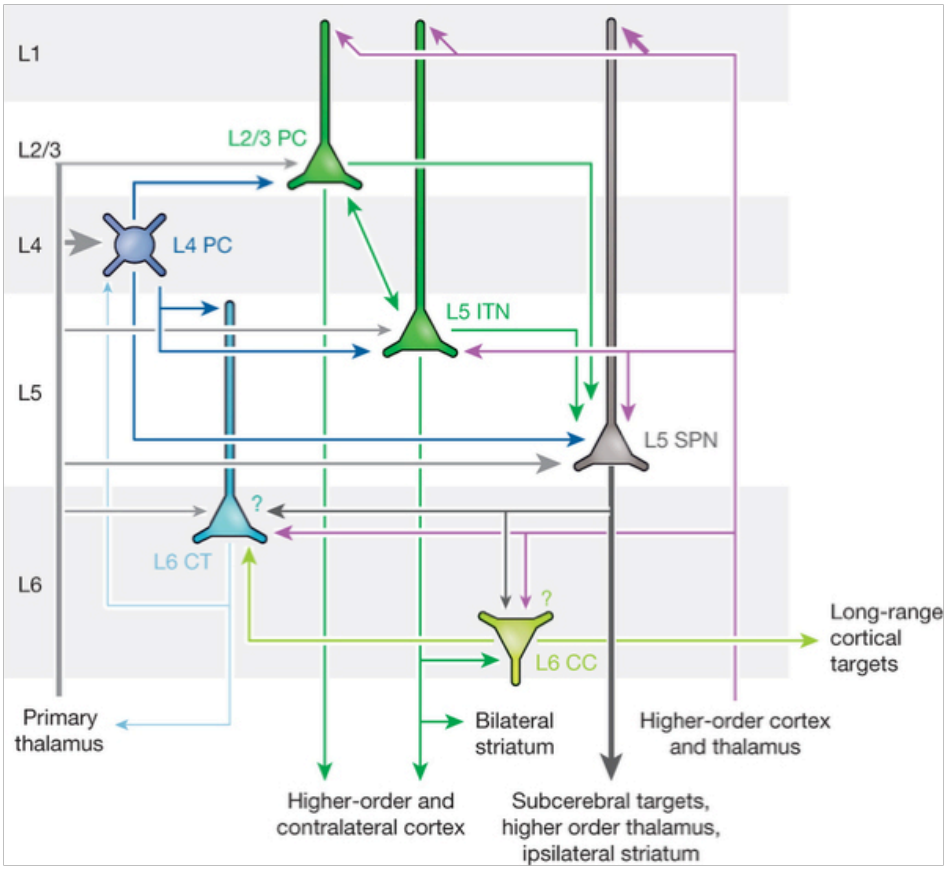

Fig 1.2 Canonical cortical circuit of primary sensory cortex. Adapted from Harris and Mrsic-Flogel, 2013 (Harris and Mrsic-Flogel 2013).

conducted in anesthetized or sedated (and paralyzed) animals. More recently, the field is moving towards studying S1 sensory processing in awake, behaving animals. Studies done in this manner have shown that spiking activity of barrel cortex neurons in all layers are only weakly modulated by active whisking, and only L5a cells show significant increase in firing during active whisking (de Kock and Sakmann 2009). In another study where mice were taught to perform an object localization task, L4 and L5 neurons show the most increase in spiking responses to object contact (O'Connor, Peron et al. 2010).

Sparse coding in L2/3 in barrel cortex

Recordings in both anesthetized as well as awake animals revealed that unlike 4 and 5, L2/3 pyramidal neurons display remarkable sparse spiking activity. Spontaneous firing rates of L2/3 cells measured in anesthetized and awake quiescent animals were well below 1 Hz (Brecht, Roth et al. 2003, Kerr, Greenberg et al. 2005, de Kock and Sakmann 2009). Passive whisker stimuli applied to the PW evoke substantial subthreshold depolarizations in L2/3 neurons, but only rarely elicit any suprathreshold spiking responses (Brecht, Roth et al. 2003). We recently showed that presenting complex spatial-temporal patterns of whisker stimulation optimized for individual neurons strongly engages neurons in L4-6, but not L2/3 (Ramirez, Pnevmatikakis et al. 2014). Studies in awake animals show that L2/3 spiking activity does not increase with active whisking in air, and is only weakly facilitated during active object contact (O'Connor, Peron et al. 2010, Crochet, Poulet et al. 2011, Sachidhanandam, Sreenivasan et al. 2013). The sparseness is unevenly distributed within L2/3 cell population with only 10% of the neurons generating the majority of spiking activity under most circumstances (Kerr, Greenberg et al. 2005, Yassin, Benedetti et al. 2010, Crochet, Poulet et al. 2011).

Several studies have aimed to shed light on the cellular and circuit mechanisms underlying sparse activity in L2/3. The results show that during active touch, L2/3 receives feed forward excitation from L4 via the lemniscal pathway and feed forward inhibition from local GABAergic neurons. The mixed synaptic currents give rise to a characteristic synaptic reversal potential that is just below the spiking threshold of these cells (Crochet, Poulet et al. 2011). This renders the neurons silent even though they receive significant subthreshold depolarization. This result strongly suggests that feed

forward sensory inputs through the lemniscal pathway are simply not enough to engage L2/3 pyramidal neurons. Given that L2/3 receives inputs from other higher order brain regions, it is likely that L2/3 activity could be unleashed by engagement of one or more of these inputs.

Due to their sparse activity, the functional role of L2/3 neurons in sensory processing remains elusive. However, in vitro studies have shown that L2/3 neurons form strong driving synapses onto L5 pyramidal neurons, the main output neurons of S1 (Oberlaender, de Kock et al. 2012). Due to their projection to various subcortical regions, L5 neuronal activity were thought to be able to strongly influence behavioral responses to sensory inputs (Znamenskiy and Zador 2013). Therefore, activation of L2/3 can have profound impact on both sensory processing and the subsequent behavior.

1.3 SOURCES OF TOP-DOWN INPUTS IN THE RODENT BARREL CORTEX

Every primary sensory cortex receives many top-down higher order inputs in addition to the thalamic inputs that directly convey sensory messages. These inputs are thought to convey information about the animal's attentional states, and to mediate integration of the non-sensory contextual information with modality-specific sensory inputs. As mentioned above, most long-range inputs from higher-order brain regions reside in L1 as well as the infragranular layers of primary sensory cortices (Veinante and Deschenes 2003, Wimmer, Bruno et al. 2010). The rodent barrel cortex receives top-down inputs from various motor, higher-order sensory, and neuromodulatory brain regions (Cauller, Clancy et al. 1998). Here we discuss three of the most prominent sources of top-down long-range axons in barrel cortex: POm, M1, and S2.

The posterior medial thalamus

POm, as mentioned in a previous section, is the thalamic nucleus of the paralemniscal pathway in the rodent sensory system. Unlike VPM, POm requires large amplitude, multi-whisker stimulation to elicit any spiking response. Even then, POm responses are weak, inconsistent, and with long latency. Anatomical and physiological studies have demonstrated that POm receives driving inputs from both the SP5i as well as S1 L5 corticothalamic neurons (Trageser and Keller 2004, Groh, Bokor et al. 2013). Therefore, POm can potentially assume either the role of a primary thalamic sensory

nucleus (relaying sensory information from the periphery), or that of a higher-order thalamic nucleus (modulating information flow between cortical regions). Evidence points to cholinergic modulation of subthalamic nucleus zona incerta (ZI), a source of strong feed forward inhibition to all high order thalamic nuclei, for switching the flow of information in POm (Trageser and Keller 2004). Under anesthesia or light fentanyl sedation, POm activity is chronically inhibited by GABAergic input from the zona incerta (ZI). Cholinergic input from the PPT inhibits ZI activity, and in turn disinhibits POm. Upon ZI inactivation, POm neurons that receive peripheral inputs were able to respond robustly to whisker stimuli at much shorter latencies (Trageser and Keller 2004, Trageser, Burke et al. 2006). These results suggest that ZI regulates POm transmission of peripheral sensory information under different behavioral conditions.

In the last decade or so, a theory emerged which links POm neurons to pain perception. A subpopulation of POm neurons have also been shown to be high responsive to painful stimulation to the whisker pad (Masri, Quiton et al. 2009, Frangeul, Porrero et al. 2014). However, it is unclear from the evidence whether they are responsive exclusively to noxious stimuli, or a wide variety of behaviorally salient stimuli. Our existing knowledge about POm neurons suggests that POm activity is closely modulated by the animal's behavioral state (level of alertness, salience of a given stimuli). Given the right circumstances, POm can provide robust sensory inputs to barrel cortex.

POm thalamocortical axons ramify in both L1 and L5a of barrel cortex. Previous investigations have shown that POm axons form functional synapses onto both L2/3 and L5a pyramidal neurons in S1 while avoiding L5b pyramidal neurons (Petreanu, Mao et al. 2009). Recent anatomical studies have shown that POm can be subdivided into

anterior and posterior subnuclei, where the neurons in anterior POm preferentially innervate L5a and the posterior POm is more likely to innervate L1 (Ohno, Kuramoto et al. 2012). It is possible that inputs to these different layers are conveying different sensory information, however, the receptive field properties of neurons in these anatomical sub-nuclei are currently unknown.

Primary Motor Cortex

The vibrissal representation of the rodent M1, like the barrel region of S1, is disproportionately large. Direct electrical stimulation of vibrissal M1 elicits whisker movements (Brecht, Krauss et al. 2004, Haiss and Schwarz 2005). However, recordings from awake, actively whisking animals show that M1 neurons do not encode whisking behavior cycle-by-cycle. Instead, M1 firing rate increases just before the beginning of a whisking bout (Carvell, Miller et al. 1996, Friedman, Jones et al. 2006). In fact, rodents retain their ability to whisker after M1 aspiration (Gao, Hattox et al. 2003). M1 activation, therefore, is thought to be responsible for initiation and modulation of whisking behavior, whereas actual rhythmic whisking cycles are generated subcortically. Recent studies have identified the neurons in the intermediate band of the reticular formation in the brainstem as the central pattern generator for generating rhythmic whisking (Moore, Deschenes et al. 2013).

The vibrissal M1 and S1 are reciprocally connected (Veinante and Deschenes 2003, Ferezou, Bolea et al. 2006). M1 L5 neurons send long-range axon collaterals to barrel cortex. These axons ramify in L1, deep L5, and L6 of barrel cortex. Single-cell studies of M1 projections to barrel cortex identified two different populations of M1

barrel-projecting L5 neurons based on their final projection target of the main axon branch: 1) cortical callosal neurons that project to the contralateral cortex, and 2) corticofugal neurons that target subcortical regions. Cortical callosal neurons account for over 80% of the total S1-projecting cells. Their axons arborize in the infragranular layers of S1 and not in L1. In contrast, corticofugal neuronal axons only arborize horizontally in L1 and have no branches in L5 and 6 of barrel cortex (Veinante and Deschenes 2003). In short, similar to POm projections to S1, M1 inputs to the L1 and L5/6 likely originate from different populations of neurons and are likely transmitting very different information.

Several recent physiological studies, both in vivo and in vitro, have investigated motor cortex inputs to S1 neurons. M1 axons form functional excitatory synapses on both the apical and basal dendrites of L2/3, L5, and L6 pyramidal neurons of barrel cortex (Lee, Carvell et al. 2008, Petreanu, Mao et al. 2009, Kinnischtzke, Simons et al. 2013, Zagha, Casale et al. 2013). In supragranular layers, M1 axons preferentially recruit vasointestinal peptide-expressing (VIP) GABAergic interneurons (Kinnischtzke, Simons et al. 2013, Lee, Kruglikov et al. 2013). The VIP neurons, in turn, inhibit somatostatin-positive interneurons that directly inhibit distal apical dendrites of L2/3 pyramidal neurons (**Fig 1.3**). The main effect of M1 inputs to the superficial layers of barrel cortex, therefore, is disinhibition of the apical dendrites of L2/3 neurons (Lee, Kruglikov et al. 2013). While these studies have been extensive, they mostly focus on monosynaptic effects of minimally activating M1 axons. The overall network effects of M1 inputs on sensory processing of barrel cortex neurons is still yet to be investigated.

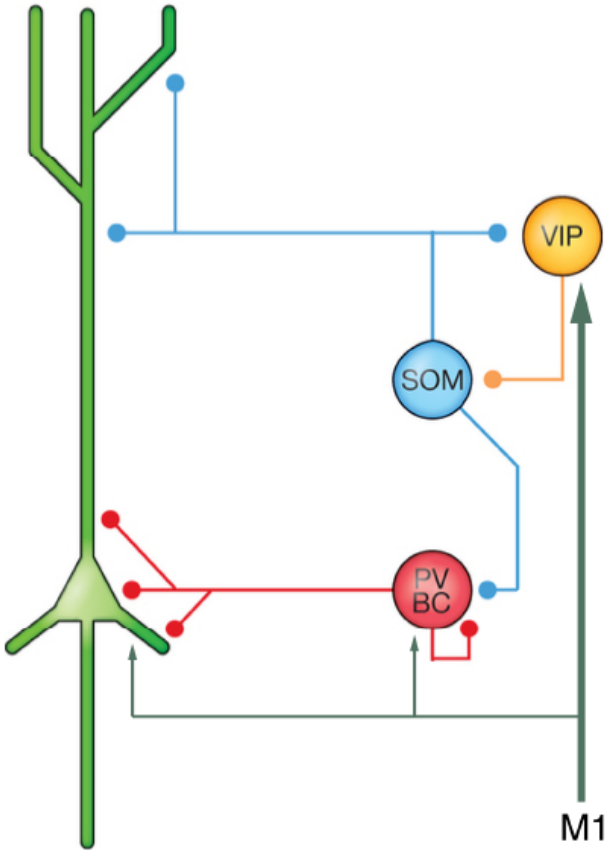

Fig 1.3 Schematic of current understanding of M1 inputs to L2/3 of primary sensory cortex. Adapted from Harris and Mrsic-Flogel, 2013 (Harris and Mrsic-Flogel 2013).

The Secondary Somatosensory Cortex

Out of the three barrel-projecting regions of focus, we know the least about the vibrissal region of S2. Anatomical and physiology experiments show that POm, instead of VPM, provides the main thalamic driving inputs in S2, and S2 receptive fields reflect this (Kwegyir-Afful and Keller 2004, Theyel, Llano et al. 2010). One *in vivo* physiological study of S2 response properties to sensory input showed that S2 neurons (in L2-6) respond with similar latencies as S1. However, S2 neurons have weaker response amplitudes, and much larger receptive fields (Kwegyir-Afful and Keller 2004). They

often respond with equal amplitudes to several PWs. The function of S2 during sensory behavior is not yet clear. Primate (both human and non-human) studies on S2 have suggested that S2 may be important for recognition and processing of noxious stimuli (Treede, Apkarian et al. 2000, Timmermann, Ploner et al. 2001). Another study done in non-human primates show that S2 can encode decision-making during sensory discrimination tasks (Romo, Hernandez et al. 2002).

Anterograde and retrograde tracer studies established that S2 and S1 are reciprocally connected (Cauller, Clancy et al. 1998, Aronoff, Matyas et al. 2010, Chen, Carta et al. 2013). S2-projecting neurons in L2/3 of S1 seem to be more engaged by whisking and contact during texture discrimination tasks than detection tasks, suggesting that S2 might be functionally involved in texture discrimination (Chen, Carta et al. 2013). However, that is the current extent of our knowledge. The functional effects of S2 feedback inputs on sensory processing of S1 neurons have not been investigated.

1.4 OVERVIEW

The purpose of this thesis is to study the effect of M1, POm, and S2 inputs on S1 sensory processing. In the next chapter, we test the hypothesis activation of top-down inputs induce enough excitatory inputs to L2/3 pyramidal neurons to boost their sensory responses. We compare the effects of activating each one of the three higher order brain regions on barrel cortex L2/3 neurons. Overall, our experiments show that POm activation induces far stronger excitatory inputs in L2/3 pyramidal neurons than activation of M1 or S2, and could have profound impact on sensory responses of L2/3 neurons.

2.0 BARREL CORTEX L1 RESPONSES TO ELECTRICAL STIMULATION OF POM, M1 AND S2

2.1 INTRODUCTION

Prior to the experiments performed in Chapter 3, I was interested in using two-photon microscopy to image calcium signals in apical dendrites of L2/3 pyramidal neurons in response to activation of L1 long-range inputs. The motivation of the project is similar to that of the project in Chapter 2: to shed light on the network influence of long-range projections from POm, M1, and S2 on L2/3 sensory processing. Many in vitro studies have demonstrated that coincidental activation of apical and basal synapses in both L2/3 and L5 pyramidal neurons can elicit large, regenerative, voltage-gated calcium channel (VGCC) dependent dendritic spikes (dAPs) in the apical trunk (Larkum, Nevian et al. 2009). These dAPs appear as large amplitude plateau potentials in the soma, and can drive firing of AP bursts. More recent studies have demonstrated that dAPs indeed occur *in vivo*. During a simple sensory-based task, coincidental activation of long-range apical inputs from M1 with basal sensory inputs due to whisker contact, can elicit dAPs in L5 pyramidal neurons *in vivo* (Xu, Harnett et al. 2012). We hypothesized that similar process occurs in L2/3, where coincidental presentations of long-range inputs via L1 and passive sensory stimulation can elicit VGCC-dependent dendritic spikes, thus boosting L2/3 sensory responses.

To test this hypothesis, we proposed to perform an in vivo two-photon imaging experiment where we 1) fill a single L2/3 neuron using patch-clamp recording with a pipette filled with OGB-1, a calcium indicator, and then 2) electrically activate somas of neurons in barrel cortex-projecting regions such as POm, M1, and S2 while stimulating the PW, and 3) image the calcium responses in the apical dendritic tree of the filled

neuron. However, prior to performing the proposed experiment, we carried out several preliminary experiments to ensure that we can properly target the different barrel-projecting regions and find the topographically aligned sub-region in each area: we recorded LFPs in L1 or barrel cortex while electrically stimulating POm, M1, and S2. The next section is a summary of the data collected in these preliminary experiments.

2.2 SUMMARY OF RESULTS

All experiments described in this chapter are performed in mice.

Identification of Aligned Cortical and Subcortical Regions

The first step to these experiments is to find the aligned cortical and subcortical regions in M1, S2, and POm to position the stimulating electrode. Each of these regions has been shown to be reciprocally connected with S1 in a topographical manner (i.e. barrel column of one PW is more likely to form reciprocal connections with regions in M1, S2, or POm which represent the same whisker).

POm stimulation site is generally targeted by mapping for VPM based on the stereotaxic coordinates, and then moving the electrode ~400-500mm medial of the mapped site. Because of the weak and multi-whisker nature of POm receptive fields, it is very difficult to identify a proper PW. Therefore, the selected stimulation site usually has a receptive field that is roughly centered on the same row as the PW we are trying to target.

S2 stimulation sites were easily identifiable using intrinsic imaging. When the imaging field is wide enough to include a region more lateral than barrel cortex, one can observe two hot spots when periodically stimulating a single whisker: one for the corresponding barrel column, and the other for the S2 column (**Fig 2.1A**). We then simply identify the S2 location based on the local vasculature and position the stimulating electrode thusly.

M1 stimulation site proved to be the most difficult to locate. We first tried mapping M1 by electrically stimulating M1 and try to induce whisking. However, stimulation sites found this way often do not induce any significant LFP responses in S1. The scope of M1 in rodents is fairly ill-defined. There are evidence for the existence of more than one whisker-related regions in M1. How S1-projecting neurons are located within these sub-regions is completely unknown. We identified the stimulation site by electrically stimulating L1 of barrel cortex while performing flavo-protein imaging in M1. Electrical stimulation both anterogradely activate S1→M1 inputs as well as retrogradely activage M1 barrel-projecting neurons. Flavoprotein imaging in M1 reveal a bright spot when stimulation amplitude is large enough (**Fig 2.1B, C**). Baseline of all flavoprotein measurements were decreasing due to photobleaching of intrinsic flavoprotens. The stimulating electrode is positioned in the center of the spot.

POm, M1 and S2 stimulation reliably elicit LFP responses in L1 of barrel cortex

Stimulation of POm, M1 and S2 with a monopolar mapping glass electrode with a 1ms long voltage pulse elicited clear fast LFP responses in L1. The structure of the LFPs are similar in all three cases: an initial, immediate, multi-synaptic excitatory volley followed by an inhibitory peak. The inhibitory peak is then followed by another much weaker excitatory tail. The entire response episode returns to baseline within 300ms after the onset of electrical stimulation (**Fig. 2.2A**).

The timing of the intial excitatory dip is fairly consistent across different stimulation areas (~10 ms, **Fig. 2.2A, B**). However, the amplitude is very different between regions. As stimulation intensity increased (i.e., to 15-20V), POM began to

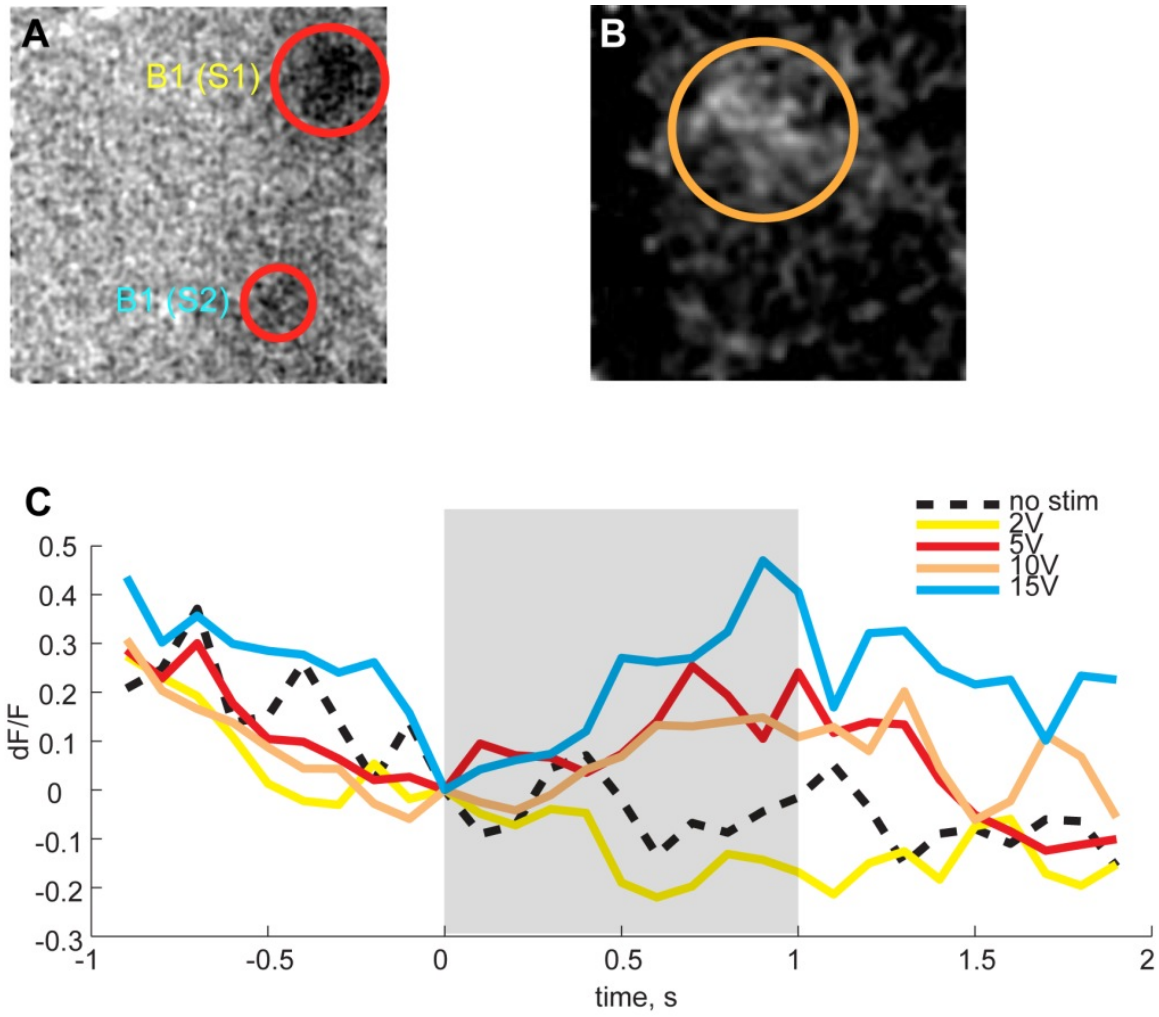

Fig 2.1 Techniques used to identify regions in S2 and M1 aligned with a single barrel column. (A) Intrinsic imaging of S1 and S2 while stimulating the B1 whisker. Red circles: peaks of intrinsic signal. (B) Flavoprotein imaging of M1 while stimulating S1 L2/3 with a monopolar glass pipette. Stimulating protocol: 10ms pulses of various voltages (5-15V) for 1s. (C) Comparison of fluorescence level at the center of identified flavoprotein hot spot under different stimulation intensities.

diverge from M1. S2 exhibited stronger responses even earlier. We became concerned that S2 stimulation was contaminated by direct activation of S1 axons and POM axons might be contaminated by direct activation of VPM axons. (**Fig. 2.2C**). Due to the nature of electrical stimulation, these results are very difficult to interpret. For this and many other reasons that will be discussed below, we decided to change course and use ChR2

mediated optogenetic methods to further investigate long-range inputs to L2/3 of barrel cortex.

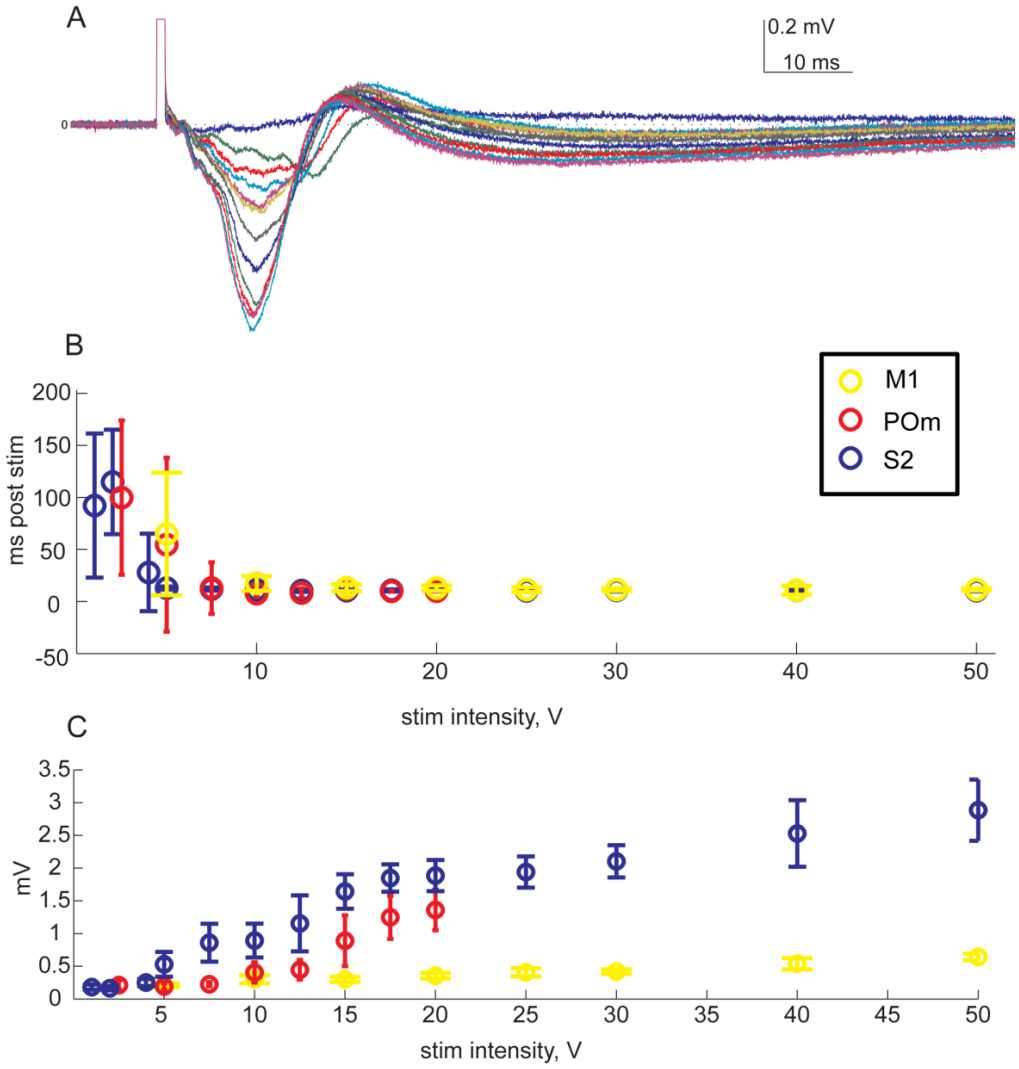

Fig 2.2 Electrical stimulation of POm, M1, and S2 somas elicit clear LFP responses in L1 of barrel cortex. (A) Example traces of M1 stimulation, intensities from 5-90V; (B) Timing of initial LFP excitatory peak vs. stimulus intensity; (C) Initial LFP excitatory peak amplitude vs. stimulus intensity.

2.3 DISCUSSION

There are several reasons for which we did not continue our efforts with this project. The most mundane reason was the simple steric hindrance experienced by trying to align stimulating electrodes with target areas (especially deep subcortical regions such as POm) while also fitting the objective used for imaging dendritic branches. Here we discuss some of the more interesting advantages of using optogenetic methods to approach this project.

Problems of electrical stimulation

While we have worked out how to target specifically aligned M1, S2 and POm regions for a defined barrel column, the process is fairly cumbersome and sometimes unreliable. Also, when electrically stimulating an area, we not only activate all the neurons nearby the tip of the electrode, but also any fibers of passage in the area. In fact, studies have shown that electrical stimulation may be more effective at activating fibers of passage than local neuronal cell bodies (Histed, Bonin et al. 2009). Therefore, when we stimulate a general region in M1, S2, or POm, we have little control of the types of neurons being activated. We are likely to be activating many non-barrel projecting neurons in these areas and therefore causing unknown secondary effects. Also, since these areas are reciprocally connected with S1, we are very likely to be backfiring projection axons from barrel cortex. Our LFP data therefore is contaminated by synaptic activities generated by the local cortical circuitry via antidromic activation of S1 neurons in L2/3 and L5.

The radius of electrical stimulation increases with the intensity of the stimulus. Therefore, the closer the stimulation site is to S1, the more likely that the LFP responses are contaminated by activation of local S1 circuitry. This is particularly tricky for S2, located within 1mm lateral to barrel cortex. This is also problematic for POm activation: because POm is located right next to VPM, any electrical stimulation of POm is at risk of also activating VPM and the lemniscal pathway.

Advantages of optogenetics

For the disadvantages listed above, we have chosen to approach the project using the methods described in Chapter 2. We infect as large of an area as we can in each of these S1-projecting regions, especially for M1 and POm, so we can cover all different sub-regions of each area. Then we directly activate the infected axon fibers by shining light in S1 as opposed to the neuronal somata, thus specifically activating only neurons from these regions that actually project to S1.

Though not applicable for the project in Chapter 2, there are other important advantages of optogenetic methods. In genetically modified mouse lines, one can obtain cell-type as well as layer specific expressions of ChR2, thus providing even more control of the stimulation, and therefore more clearly interpretable outcomes. For these and other reason, we, along with the rest of the field, have chosen to use optogenetics as the preferred method for functional circuit and network dissection.

2.4 Method

Intrinsic imaging

To image intrinsic signals, the thinned skull was obliquely illuminated with filtered (630 nm) light from a power-stabilized halogen lamp. A single whisker was deflected by a piezo three times for 100 ms with 100-ms pauses. Fifty movies (3,000 frames each) were recorded at 500 Hz by using a 4×/0.1 NA objective (Zeiss) and averaged. The interstimulus interval was 30 s. An image was taken under 510-nm illumination to record the blood vessel pattern. The sensory-evoked map of the barrel positions superimposed on the vasculature image was used to position stimulating electrodes.

Flavoprotein imaging

To image flavoprotein autoflorescence, the thinned skull was obliquely illuminated with filtered (510 nm) light from a power-stabilized halogen lamp. A glass unipolar electrode (5μm diameter) was place in L5 (1500 μm) of an identified barrel. We stimulated S1 with 10ms pulses of various voltages (5-15V) for 1s, with 50 pulses per second. Fifty movies (1,500 frames each) were recorded at 500 Hz by using a 4×/0.1 NA objective (Zeiss) and averaged. Onset of the electrical stimulation is set at 1second after the onset of imaging. The interstimulus interval was 5 s.

3.0 LAYER 2/3 OF S1 IS MORE STRONGLY ACTIVATED BY HIGHER-ORDER THALAMUS THAN HIGHER-ORDER CORTEX

3.1 ABSTRACT

Layer (L) 2/3 pyramidal neurons of the primary somatosensory cortex (S1) are sparsely active, spontaneously and in response to sensory stimuli. Long-range inputs from higher-order areas may be required to engage L2/3 neurons. We investigate the *in vivo* impact of long-range axons on L2/3 pyramidal neurons by expressing channelrhodopsin in each of the three main feedback pathways to S1: the primary motor cortex, the secondary somatosensory cortex, and the secondary somatosensory thalamic nucleus (the posterior medial nucleus, POm). The projections from the higher-order cortical areas were relatively weak. POm however robustly depolarized L2/3 cells and, when paired with peripheral stimulation, evoked suprathreshold responses. POm triggered not only a strong fast-onset depolarization but also a delayed persistent response lasting up to 1 second. Silencing POm abolished the persistent but not initial response, indicating a recurrent circuit mechanism. We conclude that second-order thalamus affords a powerful and sustained means for ungating L2/3, perhaps during active sensory behavior.

3.2 INTRODUCTION

Layer (L) 2/3 pyramidal neurons of the primary sensory cortices exhibit sparse activity both spontaneously and in response to sensory stimuli (Barth and Poulet 2012). Even in awake animals performing tactile detection tasks, L2/3 firing probability remains low and is substantially lower than that of most other cortical layers (O'Connor, Peron et al. 2010). Patch-clamp recording of L2/3 pyramidal neurons in the whisker representation of rodent S1, or the barrel cortex, during active whisking revealed that sensory inputs reliably evoke fast onset depolarizing subthreshold responses in L2/3 neurons (Crochet, Poulet et al. 2011, Sachidhanandam, Sreenivasan et al. 2013). However, sensory input also engages strong feed-forward inhibition, which keeps membrane potential (V_m) of most L2/3 neurons below spike threshold, rendering them quiet or only sparsely responsive (Crochet, Poulet et al. 2011). This phenomenon suggests that sensory information arriving in L2/3 via the lemniscal pathway (Thalamus→ L4 → L2/3) alone is insufficient to drive L2/3 activity. In accordance with this, we recently showed that presenting complex spatial-temporal patterns of whisker stimulation optimized for individual neurons strongly engages neurons in L4-6, but not L2/3 (Ramirez, Pnevmatikakis et al. 2014).

Excitatory inputs from other brain regions, perhaps activated under specific behavioral conditions, may be required to engage L2/3. L2/3 neurons in primary somatosensory cortex (S1) receive functional top-down inputs from higher-order cortical and subcortical regions such as the primary motor cortex (M1) (Veinante and Deschenes 2003, Petreanu, Mao et al. 2009, Kinnischtzke, Simons et al. 2013, Lee, Kruglikov et al.

2013) and the secondary somatosensory nucleus of the thalamus, called the posterior medial (POm) nucleus (Lu and Lin 1993, Rubio-Garrido, Perez-de-Manzo et al. 2009, Ohno, Kuramoto et al. 2012). Previous studies of these long-range inputs have been mainly focused on the monosynaptic effects of minimally activating M1 or POm inputs in S1. The network effect of these long-range inputs on S1 L2/3 neurons has not been investigated. Additionally S1 receives significant input from the secondary somatosensory cortex (S2), whose effects remain largely unexplored (Cauller, Clancy et al. 1998).

We set out to investigate if top-down inputs from higher order brain regions could ungate L2/3 activity using a combination of optogenetic and *in vivo* whole-cell recording. We focused on the three main barrel-cortex projecting regions: M1, POm, and S2. We discovered that POm activation elicited significantly stronger depolarizations in L2/3 neurons than M1 and S2. POm input was robust enough to boost sensory responses of L2/3 neurons in both anesthetized and lightly sedated animals. Furthermore, POm activation in awake and sedated animals elicited delayed long lasting depolarizations in L2/3, suggesting POm may profoundly impact S1 sensory processing during behavior.

3. 3 RESULTS

Laminar distributions of M1, S2, and POm axons

To compare long-range M1, S2, and POm inputs to rat barrel cortex, we injected an adeno-associated virus expressing a fusion protein of channelrhodopsin (ChR2) and yellow fluorescent protein (YFP) into each of these three areas. Three to four weeks post-injection, there was intense ChR2-YFP expression in the infected areas (**Fig. 3.1a**, bottom). In all cases, labeled axons were observed in barrel cortex, with significant innervation of L1. Axonal distributions across deeper layers varied based on the area of origin (**Fig. 3.1a**, top): POM axons were concentrated in L4 septum and L5A; M1 axons resided mostly in deep L5B and L6; and S2 axons formed bands in both L5 and L6 (**Fig. 3.1b**). Axons from all three regions avoided L4 barrels and were fairly rare in L3. To control for possible retrograde labeling we inspected barrel cortex after viral injections in POM, M1, and S2. Even after immunohistochemical amplification, no labeled somata were observed in barrel cortex.

POm more strongly depolarizes L2/3 than M1 or S2 does

To assess the relative efficacies of these long-range inputs to barrel cortex, we performed *in vivo* whole-cell recording in L2/3 barrel cortex pyramidal neurons to measure the postsynaptic responses evoked by photo-activation of ChR2-YFP-positive axons in the proximity of the patched cells (**Fig. 3.2a**). Photo-activation (10-ms pulse) of long-range fibers elicited either fast onset excitatory postsynaptic potentials (EPSPs) or

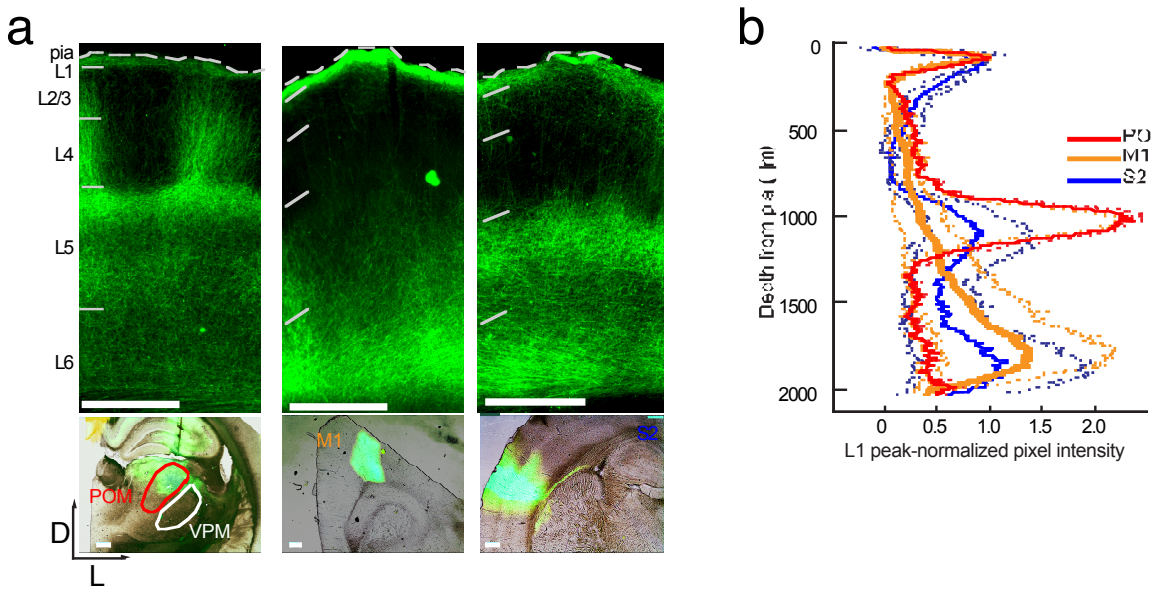

Figure 3.1 Layer 1 is one of the main layers innervated by long-range projection axons from POM, M1 and S2. (a) Top panel: labeling of long-range projection axons with ChR2-eYFP from POM (left), M1 (center), and S2 (right) shown in coronal sections of barrel cortex. Bottom: Sites of virus infection in POM (left), M1 (center), and S2(right). Scale bars: 500mms top and bottom. D, dorsal; L, lateral. (b)Average laminar profile of ChR2-eYFP labeled axons in barrel cortex. Pixel intensity was measured only for barrel-related columns (not including septal regions) and normalized to peak (n = 4 for each infected region; error bar shows ± s.e.m).

no discernable responses in most neurons recorded (example cells, **Fig. 3.2b**). Photoactivation of POM axons elicited substantial EPSPs in the majority of the neurons recorded (mean ± SEM, 2.7 ± 3.59 mV; **Fig. 3.2c**). By comparison, M1 and S2 inputs on average produced significantly smaller responses in L2/3 pyramidal neurons (M1, 0.15 ± 0.95 mV; S2, 0.87 ± 1.07 mV; one-way ANOVA, $p < 10^{-5}$; **Fig. 3.2c, d**). To control for possible cortical changes secondary to POM infection, we compared basic electrophysiological properties of cortical neurons. Neurons recorded in POM infected animals had baseline membrane potential (V_m; **Fig. 3.2e**) and input resistances (R_{in}; **Fig.**

3.2f) similar to those in M1 and S2 infected animals, indicating that the stronger POM input was not an artifact of POM infections.

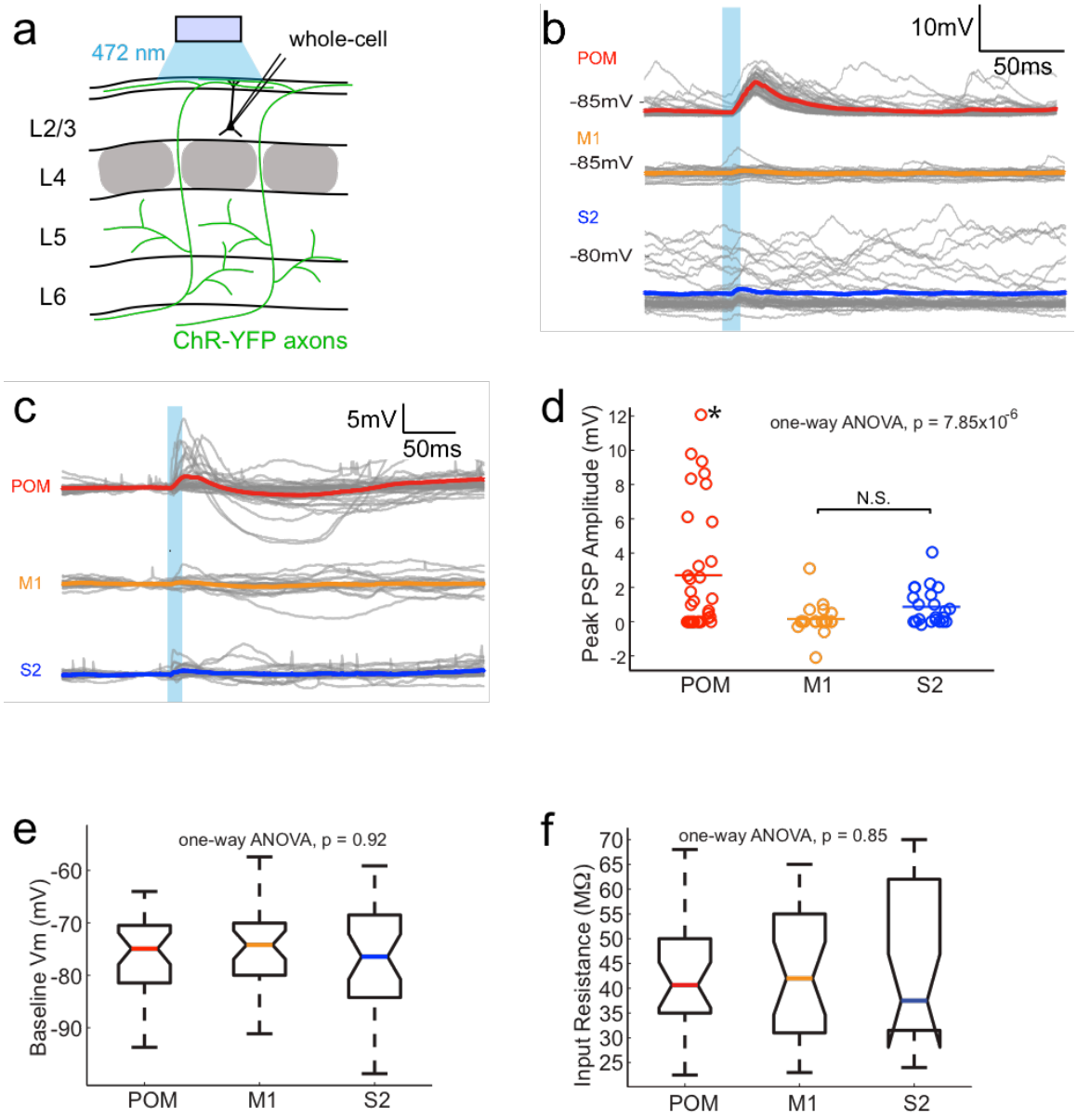

Figure 3.2 POM axons provide stronger excitatory inputs to L2/3 pyramidal neurons than M1 or S2 axons. (a) Schematic of *in vivo* ChR2 activation of long-range projection axons into barrel cortex and whole-cell recording of L2/3 pyramidal neurons. Gray, L4 barrels. (b)Example whole-cell responses of three L2/3 pyramidal neurons to photo-activating long-range axons that originated from cells infected in POM (top), M1 (middle), and S2 (bottom). Grey, 20 single trials recorded per cell; Colored, trial average. (c) Population average, baseline-subtracted responses of L2/3 pyramidal neurons to photo-activation. Grey, average responses of individual neurons

recorded, n = 33 for POM, 19 for M1, and 22 for S2. Colored, average response for each input type. (d) Distributions of peak response amplitudes to photo-activation. Activation of POM axons on average elicits a significantly larger excitatory response (mean 2.7 ± 3.6 mV) than activation of M1 (mean 0.15 ± 0.95 mV) and S2 (mean 0.87 ± 1.07 mV). One-way ANOVA, $p = 7.85\times10^{-6}$. (e)Distribution of baseline V_m of L2/3 neurons recorded. Baseline V_m did not differ based on areas of infection. One-way ANOVA, p = 0.92. (f) Distribution of resting R_{in} of L2/3 neurons recorded. Resting Rin did not differ based on areas of infection. One-way ANOVA, p = 0.85.

POM facilitates sensory responses of L2/3 pyramidal neurons

To investigate the influences of long-range POM, M1, and S2 inputs on sensory processing, we recorded L2/3 neuron responses to principal whisker (PW) stimulation, photo-activation of axons, or the simultaneous presentation of the two (**Fig. 3.3a**). In most cells, combined photo- and sensory stimuli elicit sub-threshold responses that were similar to the linear sum of the cell's responses to each stimuli alone, suggesting that sensory input and each of these long-range inputs are linearly integrated passively by the L2/3 neurons (**Fig. 3.3b**). We also compared the neurons' responses to the combined stimuli versus their responses to whisker deflection alone (**Fig. 3.3c**): while photo-activation of long-range axons from all three regions rarely suppressed sensory responses of L2/3 neurons, only POM projections facilitated L2/3 neurons' sensory response significantly (**Fig. 3.3d**). Neurons without discernable excitatory responses to photo-activation had no obvious impact on sensory responses (grey circles, **Fig. 3.3c**). These results raise the possibility that POM is a particularly important pathway for gating L2/3 activity.

Thalamic relay neurons are known to exhibit very different firing patterns in anesthetized versus awake animals. Under anesthesia, POM neurons maintain very low

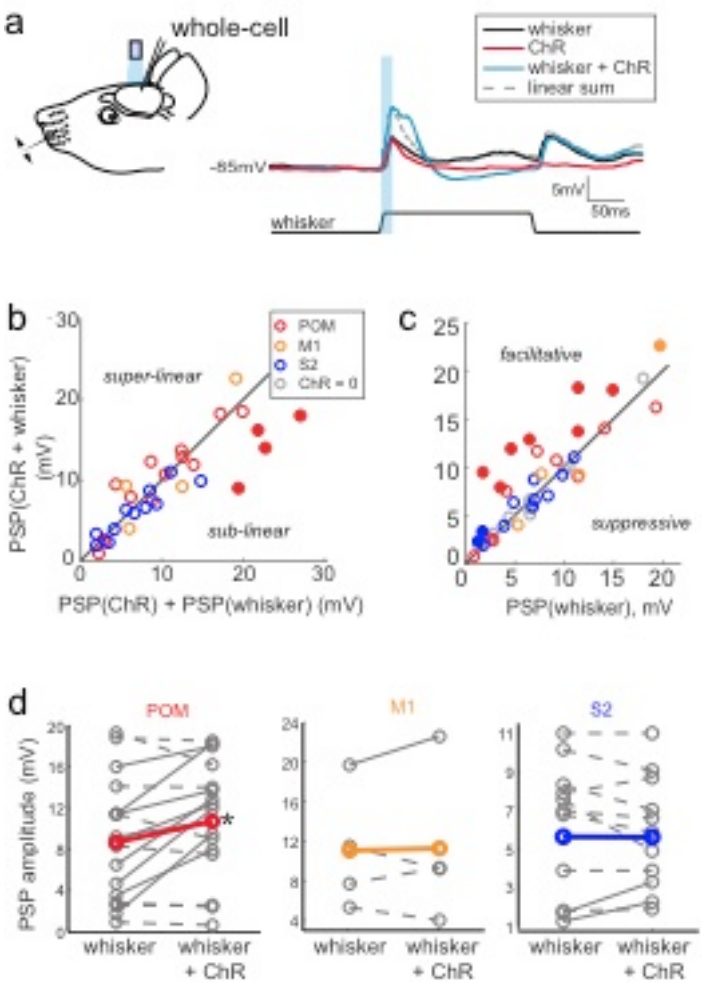

A figure 3.3 Activation of POM input facilitates sensory responses of L2/3 pyramidal neurons. (a) Left, schematic of *in vivo* ChR2 activation of long-range projection axons and whisker stimulus during whole-cell recording from a L2/3 pyramidal neuron. Right, average response of an example neuron to photo-activation alone (red), deflection of the PW (black), and simultaneous photo-activation of POM axons and PW deflection (blue). Dotted line, linear sum of PSP response to PW deflection and photo-activation. Light blue bar: 10 ms laser pulse. (b) L2/3 responses to simultaneous sensory and photo stimuli are linear. Line, linearity. Filled dots: neurons where sensory and photo-stimuli summed sublinearly. (c) Photo-activation of POM inputs to L2/3 facilitates the neurons' sensory response. (d) Summary plots. Only photo-activation of POM axons significantly facilitates sensory responses of L2/3 pyramidal neurons. (paired t-test: POM, $p = 0.027$; M1, $p = 0.86$; S2, $p = 0.95$)

firing rates (Masri, Bezdudnaya et al. 2008). Thus, POM-L2/3 synapses are likely to be completely relieved from synaptic depression when initially photo-activated under anesthetized conditions. To test for possible artifacts due to general anesthesia, we repeated the experiments using an alternative preparation in which local anesthesia is combined with opioid (fentanyl) sedation to avoid confounds of general anesthetics on

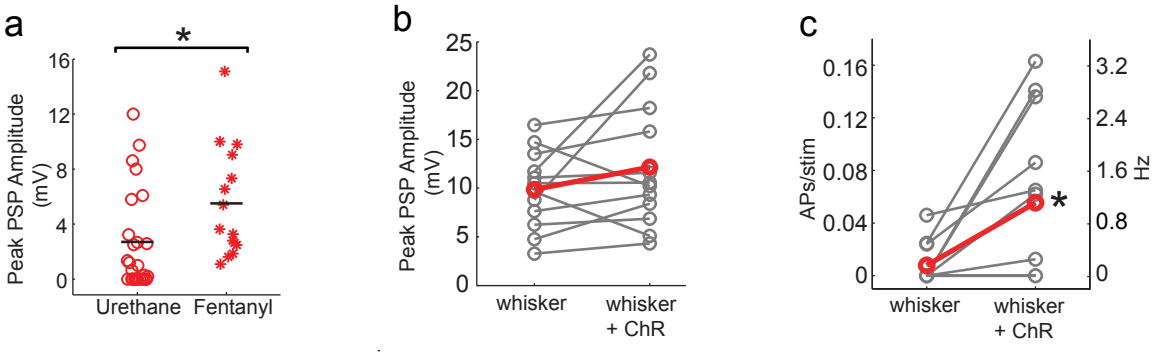

Figure 3.4 Large excitatory responses of L2/3 neurons to photo-activation of POM axons are not artifacts of general anesthesia. (a) Average L2/3 responses to photo-activation of POM axons under fentanyl sedation is even larger than those measured under urethane general anesthesia. Lines, mean. (Two-sided rank sum test, p = 0.004); (b) Under fentanyl sedation, POM axon activation slightly though not significantly boosted the sub-threshold whisker responses. Grey, individual cells; Red, mean. (Paired t-test, p = 0.16); (c) POM axon activation significantly increase spiking responses of L2/3 neurons to whisker deflection. Grey, individual cells; Red, mean. (Paired t-test, p = 0.018)

neural activity. Previous studies have shown that cortical dynamics recorded in fentanyl-sedated rats resemble those recorded in awake animals (Constantinople and Bruno 2011). ChR2-induced EPSPs were undiminished in fentanyl-sedated animals and in fact were even larger than that found in urethane anesthetized animals (**Fig. 3.4a**). Photo-activation of POM inputs under fentanyl sedation slightly boosted the sub-threshold responses of L2/3 pyramidal neurons to PW stimulation (**Fig. 3.4b**) but not statistically significantly. However, these slight subthreshold increases produced by POM translate into substantial, statistically significant increases of supra-threshold (spiking) responses of those L2/3 neurons to sensory stimuli (**Fig. 3.4c**).

We conclude that, of several long-range pathways innervating primary somatosensory cortex, POM is an unusually potent input to L2/3 pyramidal neurons.

POm persistently depolarizes L2/3 neurons under sedation and wakefulness

POm activation in sedated animals had long-lasting effects not seen in our initial anesthetized experiments. In addition to an initial fast-onset EPSP, we also observed long-lasting persistent depolarizations in L2/3 pyramidal cells in response to ChR2 activation of POM inputs (**Fig. 3.5a**). Persistent responses initiated about 150ms (mean delay, 162.8 ± 13 ms) after the onset of the light stimulation, and typically continued for over 700 ms (mean, 758 ± 133 ms; **Fig. 3.5b**). On individual trials, the persistent response showed clear periodicity in the 10-20 Hz frequency band (**Fig. 3.5a, d**). To verify that the persistent depolarization produced by this pathway is relevant for awake animals, we recorded local field potentials (LFPs) in L2/3 in awake head-fixed rats while photo-stimulating POm axons. LFP responses recorded in awake rats showed the same characteristic initial and persistent responses (**Fig. 3.5c**). Delayed persistent responses seen in LFPs recorded in awake rats showed the same onset time and duration as those in whole-cell recordings in sedated animals (compare **Fig. 3.5b** and 3.**5c**). We conclude that in anesthesia-free conditions POm is able to trigger persistent depolarization of L2/3 neurons.

Persistent responses in L2/3 require thalamic circuitry

To investigate the circuitry underlying the persistent response observed in L2/3, we juxtasomally recorded from individual POm neurons in fentanyl sedated animals while photoactivating their thalamocortical axons in barrel cortex (**Fig. 3.6a** and **3.6b**). We compared how their spiking responses changed when the animals were under general

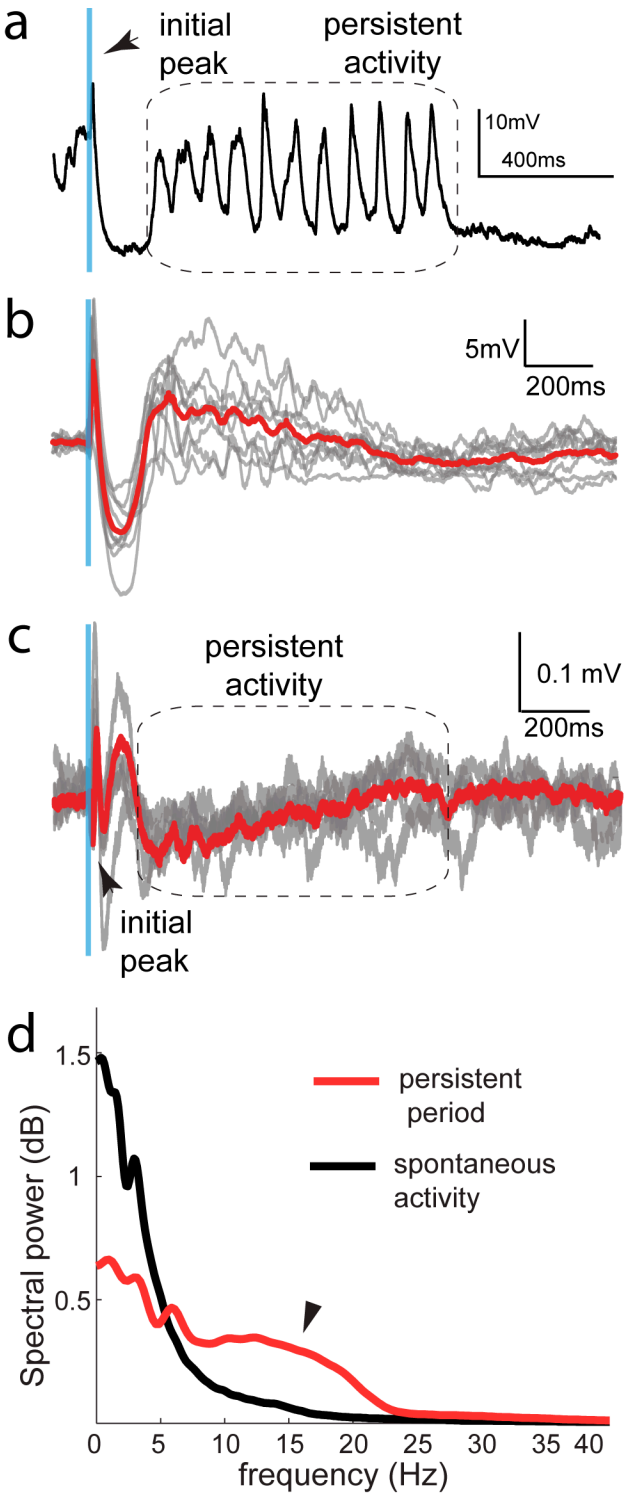

Figure 3.5 POM inputs elicit large delayed, persistent depolarization in L2/3 neurons under both sedated and awake conditions. (a) Example recording (single trial) of a L2/3 pyramidal neuron's response to a 10 ms laser pulse (blue) during fentanyl sedation. (b) Population average of L2/3 response to POM input under fentanyl sedation. Grey, average responses of individual neurons; Red, population average. (c) L2/3 LFP response to POM inputs recorded in awake rats (n = 4). Grey, average responses at each recording site. Red, population average. (d) Power-spectrum of persistent period (red) vs. spontaneous period (black) in whole-cell recordings. Arrow points to the elevated power in the 10-20 Hz frequency band observed during the persistent period.

anesthesia versus sedation by administering isoflurane to induce general anesthesia during the recording session (**Fig. 3.6b**). Consistent with previous studies (Masri, Bezdudnaya et al. 2008), spontaneous firing rate of the POm neurons increased more than ten-fold when the animal was switched from the

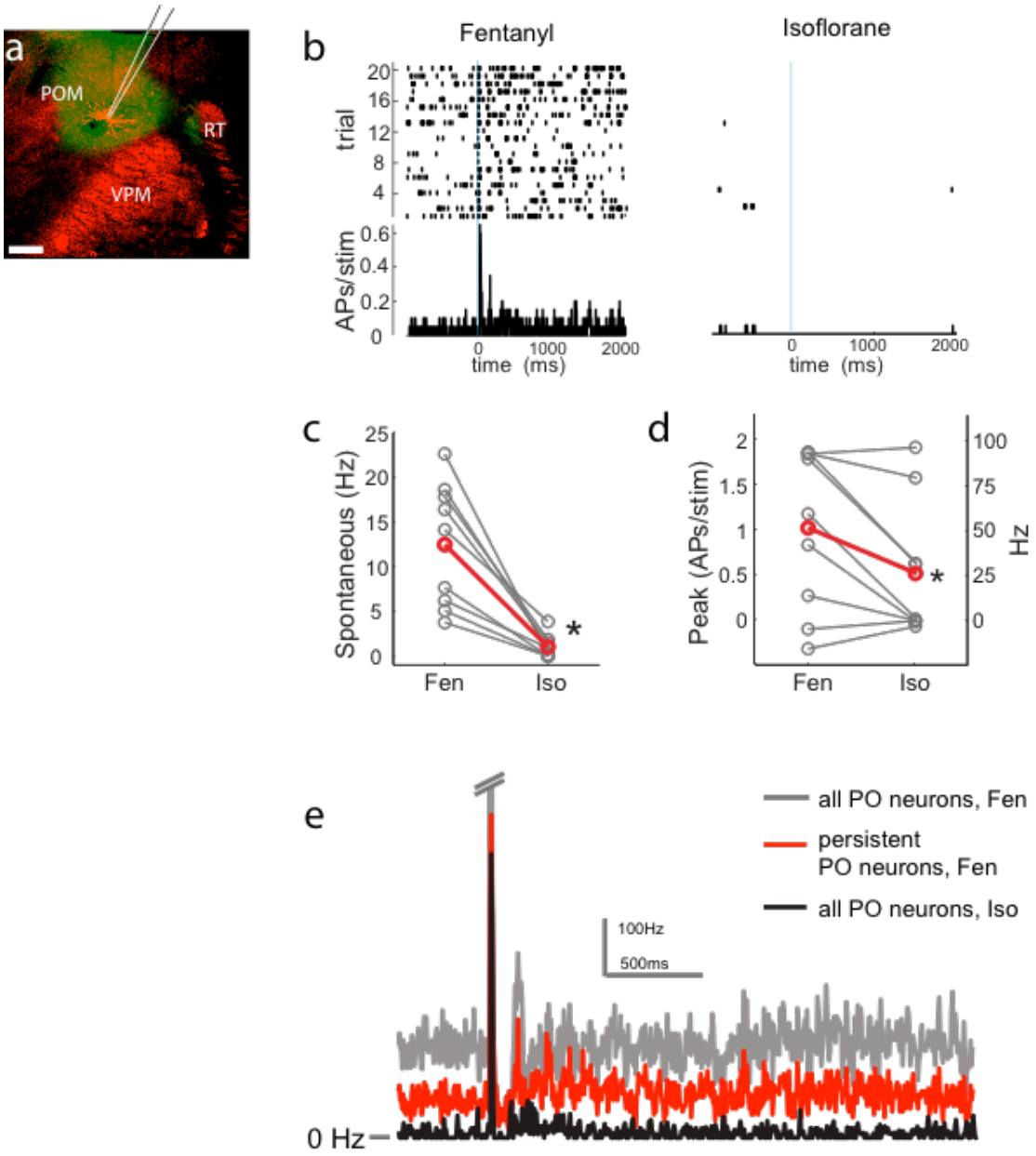

Figure 3.6 A subset of POm neurons show persistent response after photostimulation under fentanyl. **(a)** Schematic of *in vivo* juxtasomal recording and filling of POm neurons. Red, biocytin-Alexa594. Green, ChR2-YFP. **(b)** Raster plot (top) and PSTH (bottom) of a POm neuron's response to photo-stimulation of ChR2-positive cortical-projecting axons. Left, recorded under fentanyl sedation; Right, same cell but under isoflurane general anesthesia. Light blue line, 10-ms laser stimulation. **(c)** POm firing rate is significantly lower under general anesthesia than under fentanyl sedation. Grey, individual cells; Red, mean. (Paired t-test, $p = 8x10^{-4}$)**; (d)** Photo-activation of POM cortical-projecting fibers elicits more antidromic spikes in POM under Fentanyl than under isoflurane. Peak firing rate is baseline-corrected by subtracting spontaneous

firing rate measured in the pre-laser period. Grey, individual cells; Red, mean. (Paired t-test, p = 0.091) **(e)** Population PSTH of POM neurons' response to photoactivation. Grey, all POM neurons under fentanyl sedation; Red, 5 POM neurons which displayed persistent activation under fentanyl; Black all POM neurons under isoflurane.

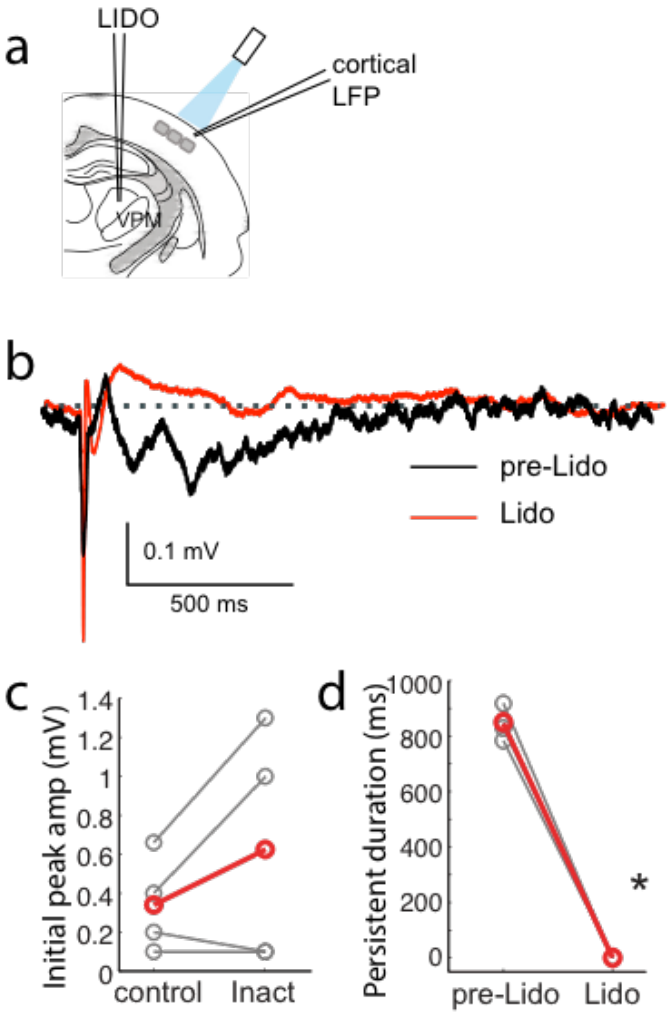

Figure 3.7 Pharmacological inactivation of POM abolishes persistent but not the initial response in L2/3 Schematic of POM inactivation experiment: While photoactivating POM cortical-projecting fiber and recording cortical LFP responses to photoactivation in L2/3, we inject 10% lidocaine or 1mg/ml muscimol through a pipette that was previously positioned in POM. (a) Population average of L2/3 LFP responses to POM input before (black) and after (red) inactivation. (b) Pharmacological inactivation slightly increased the magnitude of initial response in L2/3 (paired t-test, p = 0.24). Grey, individual animals; red, population average. (c) Persistent response in L2/3 was abolished after lidocaine injection (paired t-test, $p < 10^{-4}$). Grey, individual animals; red, population average.

anesthetized to sedated state (fentanyl mean ± SEM, 13.2 ± 8.7 Hz; isoflurane mean ± SEM, 1 ± 1.3 Hz; paired t-test, $p = 8 \times 10^{-4}$; n = 9; **Fig. 3.6c**). POm spiking responses to photostimulation also increased under sedation (paired t-test, p = 0.09; **Fig. 3.6d**), reflecting the overall increase in excitability of thalamic neurons under sedation. This

increase in evoked response likely explains how L2/3 responses to light activation of POM fibers under sedation remained strong in spite of the plausible ongoing synaptic depression. Five out of nine POM neurons recorded displayed significant persistent activation in response to light activation (**Fig. 3.6e**).

This persistent activation could result from unique synaptic or axonal properties (Sheffield, Best et al. 2011), recurrent circuits within L2/3, or circuitry involving thalamus. To test if POm is necessary for generating delayed persistent responses in L2/3, we recorded light-elicited cortical LFP responses in L2/3 barrel cortex while injecting either 10% lidocaine (2 out of 4 animals) or 1mg/mL muscimol in sterile saline (2 out of 4 animals) in POm (**Fig. 3.7a**). We found that the initial response in L2/3 remained intact, if not slightly larger during pharmacological inactivation (**Fig. 3.7b, c**). The delayed persistent response, however, is completely wiped out upon POm inactivation (**Fig. 3.7b, d**). This strongly suggests that the delayed persistent response in L2/3 is generated through either intra-thalamic or thalamocortical circuit involving POm, and is not an intracortically generated phenomenon.

3.4 DISCUSSION

We have investigated three prominent intracortical and thalamocortical projections to the rat barrel cortex: POm, M1 and S2. The laminar distribution of POm and M1 axons projecting to barrel cortex in our data are consistent with previous observations (Veinante and Deschenes 2003, Ohno, Kuramoto et al. 2012, Kinnischtzke, Simons et al. 2013). While S2 and S1 are known to be reciprocally connected, the laminar distribution of S2 axons in barrel cortex had not been previously examined in detail. Our study provides a direct anatomical comparison of these long-range barrel cortex projections. We find that these three long-range projections differ in their infragranular targets. POm, S2 and M1 axons seemingly tile L5, from shallower (closer to L4) to deeper (closer to L6) respectively; S2 and M1 axons are also both present in L6. The S2 zone appears to correspond to the region of L5/6 that lacks POm and VPM innervation (Wimmer, Bruno et al. 2010). These results suggest that within L5 and 6, there potentially exist several sub-networks that receive and integrate information from different cortical and subcortical regions.

POm can be subdivided into anterior and posterior subnuclei, which preferentially innervate L5 versus L1 of barrel cortex, respectively (Ohno, Kuramoto et al. 2012). Similarly, in M1, L5 cortico-callosal cells send projection axons, which ramify mainly in L5 and 6 of barrel cortex, whereas corticofugal cells send collateral fibers to L1 of barrel cortex (Veinante and Deschenes 2003). It is unknown if these subregions and cell types

receive differential inputs or have distinct activity patterns. We therefore targeted the injections to cover as much of each region as possible in our study. The anatomical and physiological data may reflect one kind of input or a mixture. In future studies, it would be interesting to target each sub-region or cell type separately to tease apart their individual influences on sensory processing in barrel cortex.

L2/3 pyramidal neurons in the rodent barrel cortex are sparsely active under a large range of conditions, including awake animals performing simple tactile tasks. This suggests that bottom-up sensory information from the periphery is insufficient to strongly drive L2/3 neurons, possibly resulting in L2/3 neurons employing a sparse coding strategy to represent simple tactile information. Alternatively, additional inputs such as long-range top-down inputs from various higher order cortical and subcortical regions are needed to unleash L2/3 activity. All three regions investigated in this study have axons that anatomically ramify in L1 of barrel cortex and overlap with apical dendrites of L2/3 pyramidal neurons. All three areas therefore could potentially ungate L2/3 activity. In spite of this, our data suggest that only inputs from POm are sufficient for driving L2/3 neurons and boosting their sensory responses. In contrast, M1 and S2 inputs are on average weak, having little impact. Consistent with our POm observations, a recent study of primary visual cortex in anesthetized monkeys found that pharmacological activation of pulvinar, the secondary order visual thalamic nucleus, could enhance L2/3 neuronal responses to visual stimuli (Purushothaman, Marion et al. 2012). Our data suggest that the impact of secondary sensory nuclei will be even more pronounced during behavior.

In contrast to secondary sensory thalamus, M1 appears to provide mainly strong input to inhibitory neurons in barrel cortex (Kinnischtzke, Simons et al. 2013, Lee,

Kruglikov et al. 2013). Activation of M1 can induce changes in network state of S1 through modulation of activity of inhibitory neurons (Zagha, Casale et al. 2013). Locomotion enhances L2/3 neuronal activity in mouse V1 (Niell and Stryker 2010). However, locomotion has been shown to suppress L2/3 neuronal responses in mouse primary auditory cortex (A1) (Zhou, Liang et al. 2014). The effects of locomotion on primary sensory cortices are therefore modality-dependent. Moreover, these effects may be mediated via neuromodulator release in cortex as opposed to direct M1 synapses to L2/3 (Niell and Stryker 2010, Fu, Tucciarone et al. 2014). Prior to our study, there has been little detailed investigation of S2 inputs to barrel cortex. We found that S2 provides only minor depolarizing inputs to L2/3 pyramidal neurons, perhaps slightly stronger than the contribution of M1. The S2 layers and cell types providing these inputs are unknown and should be investigated in the future.

Coincident activation of top-down apical and bottom-up basal dendrite inputs to L5 neurons can engage large calcium spiking events *in vivo,* which results in supralinear integration of the two inputs (Xu, Harnett et al. 2012). In our study, we observed only linear summation of top-down inputs (POm, M1, S2) with bottom-up sensory signals (whisker stimuli) in L2/3 pyramidal neurons, suggesting that coincident top-down and bottom-up inputs do not trigger global calcium spikes in L2/3 pyramidal neurons. Supralinearity was absent even for relatively strong top-down input, such as that provided by POm. Linear summation may partially result from the basal sensory inputs to L2/3 alone being fairly weak and unable to induce back-propagating APs that would depolarize the apical dendrites. Our results are also consistent with recent imaging studies in the somatosensory and visual systems, which showed that sensory stimulation

produces sparse local dendritic "hot spots", but not global calcium events that are indicative of the occurrences of dendritic calcium spikes (Varga, Jia et al. 2011, Palmer, Shai et al. 2014). Linear summation of these inputs also demonstrates that bottom-up L4 sensory inputs and top-down POm inputs likely innervate separate dendritic compartments (i.e., apical versus basal), whereby local depolarization by one group of synapses minimally affects the local driving force and input resistance of another dendritic compartment. Thus, despite POm, M1, and S2 having some synapses in L2/3, our data likely reflect mainly long-range synapses in L1.

During sedation and wakefulness, POm activation in our experiments could persistently depolarize cortical L2/3 pyramidal neurons for up to about 1 second. One possible explanation is that our photo-activation protocol induces isolated retroaxonal barrage firing in the distal POm cortical-projecting axons. Such barrage firing has been observed in hippocampal and cortical interneurons (Sheffield, Best et al. 2011, Suzuki, Tang et al. 2014). Our POm juxtasomal recordings exhibited no barrage firing following photo-activation. Another possibility is that persistent activity is generated by recurrent circuitry within L2/3 or between L2/3 and L5. However, our pharmacological inactivation of POm indicated that POm is necessary for generating persistent depolarization in the cortex. This rules out both retroaxonal barrage firing and purely intracortical circuit mechanisms. Since there are no known synaptic connections within POm neurons or within POm and VPM thalamic relay cells, the persistent activity is likely intrathalamic or thalamocortical loop involving POm. We observed a characteristic 10-20Hz frequency for the persistent response, which is reminiscent of oscillations like sleep spindles, generated through interactions between thalamic relay cell and the

reticular inhibitory neurons (von Krosigk, Bal et al. 1993). The persistent response we observe is likely produced by a similar circuit, mediated by POm reciprocal connections with the reticular nucleus or zona incerta.

The functional consequences of the persistent response are potentially profound. POm might not only ungate L2/3 response to sensory stimulation, but also sensitize L2/3 for prolonged periods of time thereafter. During a simple tactile detection task, the membrane potential of L2/3 pyramidal neurons in barrel cortex exhibits a prolonged depolarization. The peak of this late depolarization precedes and correlates with the behavioral choices of the animal, and optogenetic inhibition of barrel cortex during this time period interferes with behavior (Sachidhanandam, Sreenivasan et al. 2013). This late depolarization exhibits striking similarity in both timing and duration to the persistent response in our study, suggesting it too derives from POm input. If the late depolarization and the persistent response are both POm mediated, it would suggest that POm activation of cortical neurons is crucial for conscious perception of sensory stimuli.

The sensory or behavioral events triggering activity in POm, as in secondary nuclei of the visual and auditory system, are not well understood. A few earlier behavioral studies concluded that inactivation of POm neurons does not affect the animal's ability to detect passive deflection of a single whisker (Narumi, Nakamura et al. 2007). This result is unsurprising given the large, multi-whisker receptive fields of POm neurons (Diamond and Ebner 1992), as well as the fact that POm neurons receive inputs from M1 (Miyashita, Keller et al. 1994). POm neurons, therefore, are likely more engaged by behaviors that involve active sensing using multiple whiskers. At a synaptic level, POm has been demonstrated to be able to function as both a primary (driven by

peripheral inputs) and higher order (drive by top-down cortical inputs) nucleus of somatosensation (Trageser and Keller 2004, Groh, de Kock et al. 2008, Groh, Bokor et al. 2013). However, sensory responses of POm neurons have been shown to be weak due to tonic inhibition by zona incerta (ZI) (Trageser and Keller 2004). Neuromodulatory signals such as acetylcholine inhibit ZI and therefore disinhibit POm activity (Trageser, Burke et al. 2006). POm activity is potentially highly gated by attentional states, and therefore POm inputs would increase L2/3 response to tactile stimuli when the animal is highly alert and attentive.

Secondary sensory nuclei in thalamus, such as POm and pulvinar, may be important for high-order aspects of sensory processing. Lesion studies in non-human primates as well as humans have demonstrated that pulvinar is important for spatial attention and selective attention in visual search (Ungerleider and Christensen 1979, Bender and Butter 1987, Ward, Danziger et al. 2002, Wilke, Turchi et al. 2010). Behavioral studies further demonstrated that sensory responses of pulvinar neurons are strongly potentiated by heightened visual attention (Petersen, Robinson et al. 1985). Pulvinar neurons corresponding to the attended location also fire tonically at elevated levels prior to stimulus presentation, suggesting that beyond allocating spatial attention, pulvinar may also be involved in working memory (Saalmann, Pinsk et al. 2012). Few similar behavioral studies have been done to elucidate the functional role of POm. Physiological studies have demonstrated that POm sensory responses can be significantly boosted by the presence of neuromodulators, thus raising the possibility that POm activity could be strongly modulated by attention. Additionally, subsets of POm neurons are highly responsive to noxious stimuli (Masri, Quiton et al. 2009, Frangeul, Porrero et al. 2014).

However, rather than selectively representing pain, POm may respond to any stimuli of high behavioral salience. Secondary sensory nuclei in thalamus may enable encoding of such high-order contextual information during behavior (Saalmann, Pinsk et al. 2012) via the long-lasting input they provide to L2/3.

3.5 METHODS

Optogenetics

To photo-activate long-range projection fibers, female ~70-100 g Wistar rats (Charles River) were injected with adeno-associated virus (AAV1) to express a ChR2-eYFP fusion protein driven by the human synapsin promoter (AAV1.hSyn.ChR2(H134R)-eYFP.WPRE.hGH, Penn Vector Core). Standard aseptic technique was used. Rats were anesthetized with isoflurane (1-3% in O_2) and placed in a stereotax using blunt earbars. Pre-emptive systemic analgesia was administered (carprofen, 5 mg/kg, subcutaneous). Ophthalmic ointment was applied to the eyes. Rectal body temperature was maintained at 37°C with a heating pad. A small incision was made in the scalp to expose the skull overlying the target structure. The skull was thinned with a dental drill.

Craniotomies were placed stereotaxically: M1, 1.5-2.5 mm anterior to bregma and 1–2.5 mm lateral from midline (injections 500-1500 μm beneath the pia; S2, 2-3 mm posterior and 6-6.5 mm lateral (1500-2000 μm); and POm, 2.5-3.5 mm posterior and 2.5-4.0 mm lateral (4500-5000 μm). POm was targeted by physiologically locating the C and D whisker row representations in VPM and injecting 700 μm medial of these. Volumes of 60-80 nL of virus were injected over ~20 min using a Nanoject II auto-nanoliter injector (Drummond, Broomall, PA). The craniotomies were covered with bone wax, and the incision closed with absorbable sutures. Animals were allowed to recover from surgery in a clean cage with softened food palettes and water overnight before returning to their home cage.

After housing the animals for ~3 weeks (140-226 g) surgeries for physiology experiments were performed as described below. Light-activation of infected fibers was achieved by placing a 200-μm fiber optic immediately above a craniotomy over barrel cortex and delivering 10-ms pulses of 473-nm light using a DPSS laser (OEM) controlled by a mechanical shutter. Fiber output was checked between experiments using a power meter.

Animal Preparation for Physiology

In all cases, animals were initially anesthetized with isoflurane (1–3% in O_2). Body temperature was kept at 37°C by a heating blanket. Eyes were coated with lubricating ointment to prevent drying. The parietal and occipital bones were exposed, and a metal post for positioning the head was attached to the skull using dental acrylic. The parietal bone overlying left barrel cortex (centered 2.5 mm posterior to bregma and 5.5 mm lateral of the midline) was thinned with a dental drill until transparent, and small craniotomies (<0.5 mm^2) were made over the thinned region. The dura was removed.

For urethane anesthesia experiments, 74 female Wistar rats (150–250 g) were used. After the above surgery was complete, animals were administered urethane by IP injection (0.9-1g/kg). For sedation experiments, 6 rats were additionally prepared as described previously (Bruno and Sakmann 2006). Briefly, cannulae were inserted into the trachea (for mechanical ventilation), femoral artery (for blood pressure monitoring) and jugular vein (for drug infusion). Screws were inserted in the right frontal and parietal bones for electrocorticogram ("EEG") recording. All wounds were infiltrated with bupivacaine. Fentanyl (~10 μg/kg/hr) and pancuronium bromide (1.6 mg/kg/hr) were

continuously infused after discontinuation of general anesthesia, and rats were ventilated (90-100 breaths/min). Mean arterial blood pressure was typically ~120 mm Hg.

4 animals were prepared for the anesthetized-awake preparation as described previously (Constantinople and Bruno 2011). Prior to making craniotomies, screws were inserted in the right frontal and parietal bones for electrocorticogram ("EEG") recording. Instead of switching to urethane or fentanyl, animals remained on isoflurane anesthesia. Rats were wrapped in a blanket and secured in a plastic tube to reduce movement. The local anesthetic bupivacaine was regularly applied to the area of the head surrounding the acrylic. To avoid startling the rat, a black curtain was placed around the air table, and noise in the lab minimized.

Electrophysiology

Patch pipettes (4–7 MΩ) were pulled from borosilicate glass and tip-filled with (in mM) 135 K-gluconate, 10 HEPES, 10 phosphocreatin-Na_2, 4 KCl, 4 ATP-Mg, 0.3 GTP, and 0.2–0.4% biocytin (pH 7.2, osmolarity 291). Pipette capacitance was neutralized prior to break-in, and access resistance was 10–60 MΩ. Recordings were digitized at 32 kHz. Similar pipettes were used for juxtasomal recording of POm neurons. Juxtasomal pipettes were filled with 4% biocyten in aCSF (in mM: 135 NaCl, 5.4 KCl, 1.8 $CaCl_2$, 1.0 $MgCl_2$, and 50 HEPES; pH 7.2). After acquiring single-unit data, we attempt to fill the recorded neurons by injecting square current pulses (1-3 nA, 250 ms on, 250 ms off) for several minutes. LFP pipettes (2–3 MΩ) were filled with aCSF. LFPs were bandpassed 1–325 Hz.

Whisker Stimulation

Individual whiskers were deflected using multi-directional piezoelectric stimulators. Whiskers were positioned inside the stimulator ~10 mm from the base of the hair and deflected 5.7° (1-mm amplitude) using relatively high-velocity (onset and offset: ~570° / sec) ramp-and-hold movements. Deflections were applied randomly in each of eight directions, in 45° increments relative to the horizontal alignment of the rows. A receptive field was mapped by applying 10-20 blocks of such stimuli (80-160 total stimuli with 2-sec interstimulus intervals).

Immunohistochemistry

After recordings, rats were deeply anesthetized and perfused transcardially with cold 0.1 M sodium phosphate buffer (PB) followed by 4% paraformaldehyde. The left barrel cortex was cut tangentially in 100-μm sections to the white matter. The rest of the left hemisphere was sliced coronally in 100-um sections. Tangential sections were stained with streptavidin conjugated to Alexa 594 (Life Technologies) to visualize recorded neurons. In tangential and coronal sections, ChR2-eYFP signal was amplified by using a rabbit-anti-GFP primary antibody (at 1:1000, incubated overnight in 5% normal goat serum and 1% Triton-X in PB at 4 ˚C) and a goat-anti-rabbit-Alexa488 secondary antibody (at 1:200, for 2 hours in 5% normal goat serum and 1% Triton-X in PB at room temperature, Invitrogen).

Analysis

Data were analyzed using custom Matlab routines. Power analysis was performed with Chronux. DC was subtracted from V_m prior to power analysis.

4.0 GENERAL DISCUSSION

4.1 SUMMARY OF FINDINGS

In this thesis, we investigated the impact of activating higher-order long-range axons on barrel cortex L2/3 pyramidal neurons. We focused on three main sources of barrel cortex-projecting synapses: POm, M1, and S2. We found that while activation of POm axons elicits strong EPSPs in all recorded L2/3 cells, activation of M1 or S2 axons elicited small or no detectable responses. Only POM activation boosted sensory responses in L2/3 pyramidal neurons. We also found that under sedated and awake conditions, POM activation not only elicited a strong fast-onset EPSP in L2/3 neurons, but also a delayed persistent response. Pharmacological inactivation of POM abolished this persistent response but not the initial synaptic volley to L2/3. We conclude that the persistent response requires intrathalamic or thalamocortical circuits and cannot be mediated by specialized synaptic terminals or intracortical circuitry. This persistent activity may play a role in sensory processing.

4.2 EFFECTS OF TOP-DOWN INPUTS TO SENSORY PROCESSING OF L2/3 PYRAMIDAL NEURONS

M1 Inputs to L2/3 Neurons

The barrel cortex has long been known to be heavily interconnected with M1. These reciprocal connections are thought to mediate sensorimotor integration during active sensing and execution of precise motor responses to different sensory environments. M1 inputs to both excitatory and inhibitory neurons of the supragranular layers of barrel cortex have been well investigated at the circuit level (Lee, Kruglikov et al. 2013). In vitro studies have shown that M1 axons strongly recruit VIP interneurons, and only weakly innervate other interneurons and L2/3 pyramidal neurons (Kinnischtzke, Simons et al. 2013, Lee, Kruglikov et al. 2013). Activation of VIP interneurons, in turn, causes disinhibition of distal apical dendrites of pyramidal neurons in both L2/3 and L5 via direction inhibition of SOM interneurons (Pfeffer, Xue et al. 2013). This is consistent with our results where M1 activation has little depolarizing impact on L2/3 pyramidal neurons. M1 activation in L2/3 is the disinhibition of apical dendrites of pyramidal neurons, perhaps readying the neurons to receive apical inputs from other sources or preparing the apical dendrites for formations of synaptic plasticity. Recordings from awake animals also showed that active whisking or activation of M1 changes the general brain state of barrel cortex, but does not increase activity in L2/3 pyramidal neurons (de Kock and Sakmann 2009, Zagha, Casale et al. 2013). In our experiments, we only examined the influence of M1 activation on passive sensory responses on L2/3 pyramidal

neurons. Since passive sensory information arrives via L4 axons that synapse onto basal dendrites of these neurons, it is outside the influence of M1 disinhibition of the distal apical dendrites. It would be interesting to test how M1 activation would interact with other apical top-down inputs, such as POm or S2 activation.

Non-whisking related locomotion can also modulate sensory processing in L2/3. In previous studies in V1, locomotion such as running or walking has been shown to enhance V1 L2/3 activity (Niell and Stryker 2010). This effect, however, is not mediated by direct M1 inputs to V1 L2/3, but instead is induced by basal forebrain cholinergic innervation of L2/3 VIP neurons (Fu, Tucciarone et al. 2014). However, this effect is not consistent throughout all the sensory modalities. A similar study in the mouse primary auditory cortex (A1) showed the opposite effect of locomotion on A1 L2/3 neurons: locomotion actually scales down L2/3 auditory responses (Zhou, Liang et al. 2014). The specific effect of locomotion on somatosensation is not yet investigated. However, it does indicate that when studying how M1 and S1 mediate active sensing, one must consider not only the direct modulation of each cortical region on the other, but also the modality-specific neuromodulatory milieu induced by active sensing.

S2 Inputs to L2/3 Neurons

Anatomical tracing studies have demonstrated that S1 and S2 form reciprocal connections (Fabri and Burton 1991, Cauller, Clancy et al. 1998). However, prior to our study, there have not been any physiological studies examining the functional impacts of S2 inputs on barrel cortex. Our study focused on effects of S2 activation on L2/3

pyramidal neurons, and found that it is weak and ineffective at influencing L2/3 processing of passive sensory inputs. More efforts are needed to probe S2 inputs to S1 circuitry, specifically looking at the cell types and subcellular compartments targeted by S2 axons.

POm Inputs to L2/3 Neurons

The main finding of this thesis is that activation of POm inputs to barrel cortex elicits strong depolarizing inputs in L2/3 pyramidal neurons that could boost their subthreshold and spiking responses to passive sensory stimulations. Moreover, POm activation induces persistent depolarizations in L2/3 pyramidal neurons that last almost 1s after the stimulation onset. Persistent activity has been observed in prefrontal cortex and is thought to mediate working memory during delayed response tasks (reviewed in (Curtis and Lee 2010). In animals trained to perform a simple detection task, L2/3 neurons display subthreshold late depolarization that precedes the behavioral report of the animal. The amplitude of this late depolarization is strongly correlated to the animals' behavioral report (Sachidhanandam, Sreenivasan et al. 2013). The onset latency and duration of the delayed depolarization closely resemble those observed for the persistent activity elicited by POm activation. Abolishing S1 cortical activity during the late depolarization period somewhat impedes the animal's ability to complete the task. This suggests that the circuitry underlying the observed late depolarization could be crucial for sensory perception, or maintaining sensory information until the animal could make a proper behavioral report. It is unclear whether POm activation is responsible for eliciting the late depolarization observed by Sachidhanandam et. al., and more studies need to be

done to uncover the circuitry underlying this phenomenon. However, our study suggests that POm activation not only directly boost L2/3 sensory responses, is also capable of influencing S1 signal processing for prolonged periods of time after stimulus onset and can potentially be important for other cognitive aspects of sensory computation.

4.3 BROADER DISCUSSIONS AND FUTURE DIRECTIONS

Is POm a primary or higher order thalamic nucleus?

POm has long been identified as the higher order somatosensory thalamic nucleus because of 1) its ambiguous sensory receptive field, and 2) it inherits most of its sensory responses from cortex. Under anesthesia, cortical inactivation abolishes POm sensory responses completely whereas VPM receptive field remains mostly unaltered (Diamond and Ebner 1992). More recent anatomical and physiological studies shown that while all POm neurons receive descending driving inputs from cortical L5b pyramidal neurons from S1, a sub-population of POm neurons also receive strong driving inputs from the brainstem (Groh, Bokor et al. 2013). These cells are able to integrate top-down cortical inputs with peripheral sensory inputs from the brainstem, hence earning the name "integrator" POm neurons. Both populations of neurons experience tonic inhibition from ZI (Trageser and Keller 2004). However, when ZI inhibition is removed via cholinergic modulation, only the integrator neurons display strong SP5i driven sensory receptive field (Trageser and Keller 2004). Therefore, the functionality of POm could change depending on the behavioral state of the animal. For example, when the animal is not attending to

whisker-mediated stimuli, POm neurons could behave uniformly as one higher order thalamic nucleus; However, when the animal begin paying attention to tactile stimuli, POm can act as two sub-nuclei where one mostly relay ascending sensory information and the other remain cortically driven.

There is strong evidence that POm could be divided into two anatomical subnuclei based on the target layer of the neuron's cortical projection axons (Ohno, Kuramoto et al. 2012). The anterior POm neurons tend to target L5a of S1 whereas the posterior POm preferentially innervates L1. Whether these two populations of POm neurons correspond with the two functional POm neuronal groups (integrator vs. higher order neurons) is completely unknown. Currently we broadly group all POm inputs to S1 together, unaware of whether axons projecting to L1 and L5a are transmitting similar information. However, they can potentially be two completely separate and different streams of information. The next step in investigating POm sensory processing is to understand the functional inputs to anterior and posterior POm. It is crucial for our understanding of POm function, particularly the influence of POm inputs on cortical sensory processing, that we bridge this gap in our knowledge.

Secondary sensory nuclei in thalamus, such as POm and pulvinar, may be important for high-order aspects of sensory processing. Lesion studies in non-human primates as well as humans have demonstrated that pulvinar is important for spatial attention and selective attention in visual search (Ungerleider and Christensen 1979, Bender and Butter 1987, Ward, Danziger et al. 2002, Wilke, Turchi et al. 2010). Behavioral studies further demonstrated that sensory responses of pulvinar neurons are strongly potentiated by heightened visual attention (Petersen, Robinson et al. 1985).

Pulvinar neurons corresponding to the attended location also fire tonically at elevated levels prior to stimulus presentation, suggesting that beyond allocating spatial attention, pulvinar may also be involved in working memory (Saalmann, Pinsk et al. 2012). It is not hard to imagine that POm maybe serving similar roles in somatosensory processing.

What is the function of L2/3?

Under the canonical model of cortical sensory processing, the information flow is thought to be: VPM→ L4 → L2/3 → L5 →subcortical regions. This model has been constructed based on anatomical and in vitro studies of synaptic connections between different cortical layers (reviewed in (Lubke and Feldmeyer 2007). However, recent studies by our lab as well as other have slowly started to change this established understanding. Firstly, all in vivo studies of S1 L2/3 pyramidal neurons agree on the fact that these cells are show only sparse suprathreshold sensory responses, therefore unable to provide sufficient inputs to drive L5 activity (de Kock and Sakmann 2009, Yassin, Benedetti et al. 2010, Ramirez, Pnevmatikakis et al. 2014). Secondly, L4, L5b and L6 neurons respond fastest to passive whisker stimuli, several milliseconds before L2/3 response onset (Constantinople and Bruno 2013). Thirdly, a study done by our group has shown that L5b receives strong direct driving inputs from VPM, similar to L4 barrel neurons. In fact, inactivation of L4 neurons does not alter L5b responses to passive PW stimulation (Constantinople and Bruno 2013). Given these evidences, a new model of cortical circuit emerges where L4 and L5b are parallel thalamo-recipient layers. Instead

of serially processing sensory information, S1 is seemingly composed of two parallel pathways.

How L2/3 neurons fit into this new regime is a complete mystery. The findings from this thesis and other recent studies are hinting at the fact that higher-order inputs from other cortical and subcortical regions are much more important for L2/3 function than previously thought. On the input side, L2/3 is poised to receive and integrate information from different sources; on the output side, L2/3 pyramidal neurons form large numbers of strong excitatory synapses onto L5 neurons in S1. These synapses, once activated, can have a huge impact on L5 sensory processing. L2/3 neurons therefore are ideal for modulating sensory-based behavioral responses by integrating non-sensory contextual information with modality specific sensory inputs. While L5 neurons also maintain apical dendrites in L1 and can integrate higher-order inputs with bottom-up sensory information, there is evidence that L5 and L2/3 may belong to separate sub-circuits regarding certain higher order inputs (at least regarding POm) (Petreanu, Mao et al. 2009). What functions these sub-circuits may serve are unclear. More efforts are needed to find the behavioral state during which L2/3 neurons are more active to construct a more complete and comprehensive model of cortical sensory processing.

Bibliography

Aronoff, R., F. Matyas, C. Mateo, C. Ciron, B. Schneider and C. C. Petersen (2010). "Long-range connectivity of mouse primary somatosensory barrel cortex." Eur J Neurosci **31**(12): 2221-2233.

Barrett, J. N. and W. E. Crill (1974). "Influence of dendritic location and membrane properties on the effectiveness of synapses on cat motoneurones." J Physiol **293**: 325-345.

Barth, A. L. and J. F. Poulet (2012). "Experimental evidence for sparse firing in the neocortex." Trends Neurosci **35**(6): 345-355.

Bender, D. B. and C. M. Butter (1987). "Comparison of the effects of superior colliculus and pulvinar lesions on visual search and tachistoscopic pattern discrimination in monkeys." Exp Brain Res **69**: 140-154.

Bourassa, J., D. Pinault and M. Deschenes (1995). "Corticothalamic Projections from the Cortical Barrel Field to the Somatosensory Thalamus in Rats: A Single-fibre Study Using Biocytin as an Anterograde Tracer." Eur J Neurosci **7**: 19-30.

Brecht, M., A. Krauss, S. Muhammad, L. Sinai-Esfahani, S. Bellanca and T. W. Margrie (2004). "Organization of rat vibrissa motor cortex and adjacent areas according to cytoarchitectonics, microstimulation, and intracellular stimulation of identified cells." J Comp Neurol **479**(4): 360-373.

Brecht, M., A. Roth and B. Sakmann (2003). "Dynamic receptive fields of reconstructed pyramidal cells in layers 3 and 2 of rat somatosensory barrel cortex." J Physiol **553**(Pt 1): 243-265.

Brecht, M. and B. Sakmann (2002). "Dynamic representation of whisker deflection by synaptic potentials in spiny stellate and pyramidal cells in the barrels and septa of layer 4 rat somatosensory cortex." The Journal of Physiology **543**(1): 49-70.

Bruno, R. M., T. T. Hahn, D. J. Wallace, C. P. de Kock and B. Sakmann (2009). "Sensory experience alters specific branches of individual corticocortical axons during development." J Neurosci **29**(10): 3172-3181.

Bruno, R. M. and B. Sakmann (2006). "Cortex is driven by weak but synchronously active thalamocortical synapses." Science **312**(5780): 1622-1627.

Bruno, R. M. and D. J. Simons (2002). "Feedforward Mechanisms of Excitatory and Inhibitory Cortical Receptive Fields." J Neurosci **22**(24): 10966–10975.

Carvell, G. E., S. A. Miller and D. J. Simons (1996). "The Relationship of Vibrissal Motor Cortex Unit Activity to Whisking in the Awake Rat." Somatosens Mot Res **13**(2): 115-127.

Carvell, G. E. and D. J. Simons (1989). "Thalamocortical Response Transformation in the Rat Vibrissa/Barrel System." J Neurophysiol **61**(2).

Carvell, G. E. and D. J. Simons (1990). "Biometric Analysis of Vibrissal Tactile Discrimination in the Rat." J Neurosci **10**(8): 2638-2648.
Cauller, L. J., B. Clancy and B. W. Connors (1998). "Backward Cortical Projections to Primay Somatosensory Cortex in Rat Extend Long Horizontal Axons in Layer I." J Comp Neurol **390**(2): 297-310.
Chen, J. L., S. Carta, J. Soldado-Magraner, B. L. Schneider and F. Helmchen (2013). "Behaviour-dependent recruitment of long-range projection neurons in somatosensory cortex." Nature **499**(7458): 336-340.
Chiaia, N. L., R. W. Rhoades, S. E. Fish and H. P. Killackey (1991). "Thalamic Processing of Vibrissal infoormation in the Rat: II. Morphological and Functional Properties of Medial Ventral Posterior Nucleus and Posterior Nucleus Neurons." J Comp Neurol **314**: 217-236.
Constantinople, C. M. and R. M. Bruno (2011). "Effects and mechanisms of wakefulness on local cortical networks." Neuron **69**(6): 1061-1068.
Constantinople, C. M. and R. M. Bruno (2013). "Deep cortical layers are activated directly by thalamus." Science **340**(6140): 1591-1594.
Crochet, S., J. F. Poulet, Y. Kremer and C. C. Petersen (2011). "Synaptic mechanisms underlying sparse coding of active touch." Neuron **69**(6): 1160-1175.
Curtis, C. E. and D. Lee (2010). "Beyond working memory: the role of persistent activity in decision making." Trends Cogn Sci **14**(5): 216-222.
de Kock, C. P., R. M. Bruno, H. Spors and B. Sakmann (2007). "Layer- and cell-type-specific suprathreshold stimulus representation in rat primary somatosensory cortex." J Physiol **581**(Pt 1): 139-154.
de Kock, C. P. and B. Sakmann (2009). "Spiking in primary somatosensory cortex during natural whisking in awake head-restrained rats is cell-type specific." Proc Natl Acad Sci U S A **106**(38): 16446-16450.
Diamond, M. E. and F. F. Ebner (1992). "Somatic Sensory Responses in the Rostral Sector of the Posterior Group (POm) and in the Ventral Posterior Medial Nucleus (VPM) of the Rat Thalamus." J Comp Neurol **318**: 462-476.
Diamond, M. E. and F. F. Ebner (1992). "Somatic Sensory Responses in the Rostral Sector of the Posterior Group (POm) and in the Ventral Posterior Medial Nucleus (VPM) of the Rat Thalamus: Dependence on the Barrel Field Cortex." J Comp Neurol **319**: 66-84.
Diamond, M. E., M. von Heimendahl, P. M. Knutsen, D. Kleinfeld and E. Ahissar (2008). "'Where' and 'what' in the whisker sensorimotor system." Nat Rev Neurosci **9**(8): 601-612.
Dudek, S. M. and M. J. Friedlander (1996). "Intracellular blockade of inhibitory synaptic responses in visual cortical layer IV neurons." J Neurophysiol **75**(5): 2167-2173.

Fabri, M. and H. Burton (1991). "Ipsilateral Cortical Connections of Primary Somatic Sensory Cortex in Rats." J Comp Neurol **311**: 405-424.
Feldmeyer, D., V. Egger, J. Lubke and B. Sakmann (1999). "Reliable synaptic connections between pairs of excitatory layer 4 neurones within a single 'barrel' of developing rat somatosensory cortex." J Physiol **521**(1): 169-190.
Feldmeyer, D., J. Lubke and B. Sakmann (2006). "Efficacy and connectivity of intracolumnar pairs of layer 2/3 pyramidal cells in the barrel cortex of juvenile rats." J Physiol **575**(Pt 2): 583-602.
Feldmeyer, D., J. Lubke, R. A. Silver and B. Sakmann (2002). "Synaptic connections between layer 4 spiny neuron - layer 2/3 pyramidal cell pairs in juvenile rat barrel cortex: physiology and anatomy of interlaminar signaling within a cortical column." J Physiol **538**(3): 803-822.
Feng, L., O. Kwon, B. Lee, W. C. Oh and J. Kim (2014). "Using mammalian GFP reconstitution across synaptic partners (mGRASP) to map synaptic connectivity in the mouse brain." Nat Protoc **9**(10): 2425-2437.
Ferezou, I., S. Bolea and C. C. Petersen (2006). "Visualizing the cortical representation of whisker touch: voltage-sensitive dye imaging in freely moving mice." Neuron **50**(4): 617-629.
Frangeul, L., C. Porrero, M. Garcia-Amado, B. Maimone, M. Maniglier, F. Clasca and D. Jabaudon (2014). "Specific activation of the paralemniscal pathway during nociception." Eur J Neurosci **39**(9): 1455-1464.
Friedman, W. A., L. M. Jones, N. P. Cramer, E. E. Kwegyir-Afful, H. P. Zeigler and A. Keller (2006). "Anticipatory activity of motor cortex in relation to rhythmic whisking." J Neurophysiol **95**(2): 1274-1277.
Fu, Y., J. M. Tucciarone, J. S. Espinosa, N. Sheng, D. P. Darcy, R. A. Nicoll, Z. J. Huang and M. P. Stryker (2014). "A cortical circuit for gain control by behavioral state." Cell **156**(6): 1139-1152.
Furuta, T., N. Urbain, T. Kaneko and M. Deschenes (2010). "Corticofugal control of vibrissa-sensitive neurons in the interpolaris nucleus of the trigeminal complex." J Neurosci **30**(5): 1832-1838.
Gabbott, P. L. A. and P. Somogyi (1986). "Quantitative distribution of GABA-immunoreactive neurons in the visual cortex (area 17) of the cat." Exp Brain Res **61**: 323-331.
Gao, P., A. M. Hattox, L. M. Jones, A. Keller and H. P. Zeigler (2003). "Whisker motor cortex ablation and whisker movement patterns." Somatosens Mot Res **20**(3-4): 191-198.
Groh, A., H. Bokor, R. A. Mease, V. M. Plattner, B. Hangya, A. Stroh, M. Deschenes and L. Acsady (2013). "Convergence of Cortical and Sensory Driver Inputs on Single Thalamocortical Cells." Cereb Cortex.

Groh, A., C. P. de Kock, V. C. Wimmer, B. Sakmann and T. Kuner (2008). "Driver or coincidence detector: modal switch of a corticothalamic giant synapse controlled by spontaneous activity and short-term depression." J Neurosci **28**(39): 9652-9663.
Haiss, F. and C. Schwarz (2005). "Spatial segregation of different modes of movement control in the whisker representation of rat primary motor cortex." J Neurosci **25**(6): 1579-1587.
Harris, K. D. and T. D. Mrsic-Flogel (2013). "Cortical connectivity and sensory coding." Nature **503**(7474): 51-58.
Hartmann, M. J. (2011). "A night in the life of a rat: vibrissal mechanics and tactile exploration." Ann N Y Acad Sci **1225**: 110-118.
Hausser, M. and B. Mel (2003). "Dendrites: bug or feature?" Curr Opin Neurobiol **13**(382-383).
Histed, M. H., V. Bonin and R. C. Reid (2009). "Direct activation of sparse, distributed populations of cortical neurons by electrical microstimulation." Neuron **63**(4): 508-522.
Holmes, W. R. and W. Rall (1992). "Estimating the electrotonic structure of neurons with compartmental models." J Neurophysiol **68**(4): 1438-1452.
Inomata, N., T. Ishihara and N. Akaike (1988). "Effects of diuretics on GABA-gated chloride current in frog isolated sensory neurones." Br. J. Pharmacol. **93**: 679-683.
Jaquin, M. F., R. D. Mooney and R. W. Rhoades (1986). "Morphology, response properties, and collateral projections of trigeminothalamic neurons in brainstem subnucleus interpolaris of rat." Exp Brain Res **61**: 457-468.
Kawashima, T., K. Kitamura, K. Suzuki, M. Nonaka, S. Kamijo, S. Takemoto-Kimura, M. Kano, H. Okuno, K. Ohki and H. Bito (2013). "Functional labeling of neurons and their projections using the synthetic activity-dependent promoter E-SARE." Nat Methods **10**(9): 889-895.
Kerr, J. N., D. Greenberg and F. Helmchen (2005). "Imaging input and output of neocortical networks in vivo." Proc Natl Acad Sci U S A **102**(39): 14063-14068.
Killackey, H. P. and S. M. Sherman (2003). "Corticothalamic Projections from the Rat Primary Somatosensory Cortex." J Neurosci **23**(19): 7381-7384.
Kinnischtzke, A. K., D. J. Simons and E. E. Fanselow (2013). "Motor Cortex Broadly Engages Excitatory and Inhibitory Neurons in Somatosensory Barrel Cortex." Cereb Cortex.
Kwegyir-Afful, E. E., R. M. Bruno, D. J. Simons and A. Keller (2005). "The role of thalamic inputs in surround receptive fields of barrel neurons." J Neurosci **25**(25): 5926-5934.
Kwegyir-Afful, E. E. and A. Keller (2004). "Response properties of whisker-related neurons in rat second somatosensory cortex." J Neurophysiol **92**(4): 2083-2092.

Larkum, M. E., T. Nevian, M. Sandler, A. Polsky and J. Schiller (2009). "Synaptic integration in tuft dendrites of layer 5 pyramidal neurons: a new unifying principle." Science **325**(5941): 756-760.
Lee, S., G. E. Carvell and D. J. Simons (2008). "Motor modulation of afferent somatosensory circuits." Nat Neurosci **11**(12): 1430-1438.
Lee, S., J. Hjerling-Leffler, E. Zagha, G. Fishell and B. Rudy (2010). "The largest group of superficial neocortical GABAergic interneurons expresses ionotropic serotonin receptors." J Neurosci **30**(50): 16796-16808.
Lee, S., I. Kruglikov, Z. J. Huang, G. Fishell and B. Rudy (2013). "A disinhibitory circuit mediates motor integration in the somatosensory cortex." Nat Neurosci **16**(11): 1662-1670.
Lefort, S., C. Tomm, J. C. Floyd Sarria and C. C. Petersen (2009). "The excitatory neuronal network of the C2 barrel column in mouse primary somatosensory cortex." Neuron **61**(2): 301-316.
Lichtenstein, S. H., G. E. Carvell and D. J. Simons (1990). "Responses of Rat Trigeminal Ganglion Neurons to Movements of Vibrissae in Different Directions." Somatosens Mot Res **7**(1): 47-65.
Lu, S. and R. Lin (1993). "Thalamic afferents of the rat barrel cortex: a light- and electron-microscopic study using Phaseolus vulgaris leucoagglutinin as an anterograde tracer." Somatosens Mot Res **10**(1): 1-16.
Lubke, J. and D. Feldmeyer (2007). "Excitatory signal flow and connectivity in a cortical column: focus on barrel cortex." Brain Struct Funct **212**(1): 3-17.
Maltenfort, M. G., M. L. McCurdy, C. A. Phillips, V. V. Turkin and T. M. Hamm (2004). "Location and magnitude of conductance changes produced by Renshaw recurrent inhibition in spinal motoneurons." J Neurophysiol **92**(3): 1417-1432.
Maltenfort, M. G., C. A. Phillips, M. L. McCurdy and T. M. Hamm (2004). "Determination of the location and magnitude of synaptic conductance changes in spinal motoneurons by impedance measurements." J Neurophysiol **92**(3): 1400-1416.
Manns, I. D., B. Sakmann and M. Brecht (2004). "Sub- and suprathreshold receptive field properties of pyramidal neurones in layers 5A and 5B of rat somatosensory barrel cortex." J Physiol **556**(Pt 2): 601-622.
Masri, R., T. Bezdudnaya, J. C. Trageser and A. Keller (2008). "Encoding of stimulus frequency and sensor motion in the posterior medial thalamic nucleus." J Neurophysiol **100**(2): 681-689.
Masri, R., R. L. Quiton, J. M. Lucas, P. D. Murray, S. M. Thompson and A. Keller (2009). "Zona incerta: a role in central pain." J Neurophysiol **102**(1): 181-191.
Masri, R., J. C. Trageser, T. Bezdudnaya, Y. Li and A. Keller (2006). "Cholinergic regulation of the posterior medial thalamic nucleus." J Neurophysiol **96**(5): 2265-2273.

Minnery, B. S., R. M. Bruno and D. J. Simons (2003). "Response Transformation and Receptive-Field Synthesis in the Lemniscal Trigeminothalamic Circuit." J Neurophysiol **90**: 1556–1570.
Minnery, B. S. and D. J. Simons (2002). "Response Properties of Whisker-Associated Trigeminothalamic Neurons in Rat Nucleus Principalis." J Neurophysiol **89**: 40-56.
Miyashita, E., A. Keller and H. Asanuma (1994). "Input-output organization of the rat vibrissal motor cortex." Exp Brain Res **99**: 223-232.
Miyashita, T. and D. E. Feldman (2013). "Behavioral detection of passive whisker stimuli requires somatosensory cortex." Cereb Cortex **23**(7): 1655-1662.
Moore, J. D., M. Deschenes, T. Furuta, D. Huber, M. C. Smear, M. Demers and D. Kleinfeld (2013). "Hierarchy of orofacial rhythms revealed through whisking and breathing." Nature **497**(7448): 205-210.
Narumi, T., S. Nakamura, I. Takashima, S. Kakei, K. Tsutsui and T. Iijima (2007). "Impairment of the discrimination of the direction of single-whisker stimulation induced by the lemniscal pathway lesion." Neurosci Res **57**(4): 579-586.
Nelson, S., L. Toth, B. Sheth and M. Sur (1994). "Orientation selectivity of cortical neurons during intracellular blockade of inhibition." Science **265**: 774-777.
Niell, C. M. and M. P. Stryker (2010). "Modulation of visual responses by behavioral state in mouse visual cortex." Neuron **65**(4): 472-479.
O'Connor, D. H., S. P. Peron, D. Huber and K. Svoboda (2010). "Neural activity in barrel cortex underlying vibrissa-based object localization in mice." Neuron **67**(6): 1048-1061.
Oberlaender, M., C. P. de Kock, R. M. Bruno, A. Ramirez, H. S. Meyer, V. J. Dercksen, M. Helmstaedter and B. Sakmann (2012). "Cell type-specific three-dimensional structure of thalamocortical circuits in a column of rat vibrissal cortex." Cereb Cortex **22**(10): 2375-2391.
Ohno, S., E. Kuramoto, T. Furuta, H. Hioki, Y. R. Tanaka, F. Fujiyama, T. Sonomura, M. Uemura, K. Sugiyama and T. Kaneko (2012). "A morphological analysis of thalamocortical axon fibers of rat posterior thalamic nuclei: a single neuron tracing study with viral vectors." Cereb Cortex **22**(12): 2840-2857.
Palmer, L. M., A. S. Shai, J. E. Reeve, H. L. Anderson, O. Paulsen and M. E. Larkum (2014). "NMDA spikes enhance action potential generation during sensory input." Nat Neurosci **17**(3): 383-390.
Petersen, S. E., D. L. Robinson and W. Keys (1985). "Pulvinar nuclei of the behaving rhesus monkey: visual responses and their modulation " J Neurophysiol **54**(4): 867-886.
Petreanu, L., T. Mao, S. M. Sternson and K. Svoboda (2009). "The subcellular organization of neocortical excitatory connections." Nature **457**(7233): 1142-1145.

Pfeffer, C. K., M. Xue, M. He, Z. J. Huang and M. Scanziani (2013). "Inhibition of inhibition in visual cortex: the logic of connections between molecularly distinct interneurons." Nat Neurosci **16**(8): 1068-1076.
Purushothaman, G., R. Marion, K. Li and V. A. Casagrande (2012). "Gating and control of primary visual cortex by pulvinar." Nat Neurosci **15**(6): 905-912.
Rall, W. (1962). "Theory of physiological properties of dendrites." Ann N Y Acad Sci **2**(96): 1071-1092.
Rall, W. (1967). "Distinguishing theoretical synaptic potentials computed for different soma-dendritic distributions of synaptic input." J Neurophysiol **30**(5): 1138=1168.
Rall, W., R. E. Burke, T. G. Smith, P. G. Nelson and K. Frank (1967). "Dendritic location of synapses and possible mechanisms for the monosynaptic EPSP in motoneurons." J Neurophysiol **30**(5): 1169-1193.
Rall, W. and J. Rinzel (1973). "Branch input resistance and steady attenuation for input to one branch of a dendritic neuron model." Biophysical Journal **13**: 648-688.
Ramirez, A., E. A. Pnevmatikakis, J. Merel, L. Paninski, K. D. Miller and R. M. Bruno (2014). "Spatiotemporal receptive fields of barrel cortex revealed by reverse correlation of synaptic input." Nat Neurosci **17**(6): 866-875.
Romo, R., A. Hernandez, A. Zainos, L. Lemus and C. D. Brody (2002). "Neuronal correlates of decision-making in secondary somatosensory cortex." Nat Neurosci **5**(11): 1217-1225.
Rubio-Garrido, P., F. Perez-de-Manzo, C. Porrero, M. J. Galazo and F. Clasca (2009). "Thalamic input to distal apical dendrites in neocortical layer 1 is massive and highly convergent." Cereb Cortex **19**(10): 2380-2395.
Saalmann, Y. B., M. A. Pinsk, L. Wang, X. Li and S. Kastner (2012). "The pulvinar regulates information transmission between cortical areas based on attention demands." Science **337**(6095): 753-756.
Sachidhanandam, S., V. Sreenivasan, A. Kyriakatos, Y. Kremer and C. C. Petersen (2013). "Membrane potential correlates of sensory perception in mouse barrel cortex." Nat Neurosci **16**(11): 1671-1677.
Schoonover, C. E., J. C. Tapia, V. C. Schilling, V. Wimmer, R. Blazeski, W. Zhang, C. A. Mason and R. M. Bruno (2014). "Comparative strength and dendritic organization of thalamocortical and corticocortical synapses onto excitatory layer 4 neurons." J Neurosci **34**(20): 6746-6758.
Sheffield, M. E., T. K. Best, B. D. Mensh, W. L. Kath and N. Spruston (2011). "Slow integration leads to persistent action potential firing in distal axons of coupled interneurons." Nat Neurosci **14**(2): 200-207.
Simons, D. J. (1978). "Response Properties of Vibrissa Units in Rat SI Somatosensory Neocortex." J Neurophysiol **41**(3).

Smith, T. G., R. B. Wuerker and K. Frank (1967). "Membrane impedance changes during synaptic transmission in cat spinal motoneurons." J Neurophysiol **30**(5): 1072-1096.
Suzuki, N., C. S. Tang and J. M. Bekkers (2014). "Persistent barrage firing in cortical interneurons can be induced in vivo and may be important for the suppression of epileptiform activity." Front Cell Neurosci **8**: 76.
Temereanca, S. and D. J. Simons (2004). "Functional Topography of Corticothalamic Feedback Enhances Thalamic Spatial Response Tuning in the Somatosensory Whisker/Barrel System." 41(639-651).
Theyel, B. B., D. A. Llano and S. M. Sherman (2010). "The corticothalamocortical circuit drives higher-order cortex in the mouse." Nat Neurosci **13**(1): 84-88.
Thomson, A. M. and A. P. Bannister (1998). "Postynaptic Pyramidal Target Selection by Descending Layer III Pyramidal Axons: Dual Intracellular Recording and Biocytin Filling in Slices of Rat Neocortex." Neuroscience **84**(3): 669-683.
Timmermann, L., M. Ploner, K. Haucke, F. Schmitz, R. Baltissen and A. Schnitzler (2001). "Differetial coding of pain intensity in the human primary and secondary somatosensory cortex." J Neurophysiol **86**(1499-1503).
Timofeeva, E., C. Dufresne, A. Sik, Z. W. Zhang and M. Deschenes (2005). "Cholinergic Modulation of Vibrissal Receptive Fields in Trigeminal Nuclei." J Neurosci **25**(40): 9135-9143.
Trageser, J. C., K. A. Burke, R. Masri, Y. Li, L. Sellers and A. Keller (2006). "State-dependent gating of sensory inputs by zona incerta." J Neurophysiol **96**(3): 1456-1463.
Trageser, J. C. and A. Keller (2004). "Reducing the uncertainty: gating of peripheral inputs by zona incerta." J Neurosci **24**(40): 8911-8915.
Treede, R., A. V. Apkarian, B. Bromm, J. D. Greenspan and F. A. Lenz (2000). "Cortical representation of pain: functional characterization of nociceptive areas near the lateral sulcus." Pain **87**: 113-119.
Ungerleider, L. G. and C. A. Christensen (1979). "Pulvinar lesions in monkeys produce abnormal scanning of a complex visual array." Neuropsychologia **17**: 493-501.
Varga, Z., H. Jia, B. Sakmann and A. Konnerth (2011). "Dendritic coding of multiple sensory inputs in single cortical neurons in vivo." Proc Natl Acad Sci U S A **108**(37): 15420-15425.
Veinante, P. and M. Deschenes (2003). "Single-cell study of motor cortex projections to the barrel field in rats." J Comp Neurol **464**(1): 98-103.
von Krosigk, M., T. Bal and D. A. McCormick (1993). "Cellular Mechanisms of a Synchronoized Oscillation in the Thalamus." Science **261**(5119): 361-364.

Ward, R., S. Danziger, V. Owen and R. Rafal (2002). "Deficits in spatial coding and feature binding following damage to spatiotopic maps in the human pulvinar." Nat Neurosci **5**(2): 99-100.
Watanabe, H., H. Tsubokawa, M. Tsukada and T. Aihara (2014). "Frequency-dependent signal processing in apical dendrites of hippocampal CA1 pyramidal cells." Neuroscience **278**: 194-210.
White, E. L. (1979). "THalamocortical synaptic relations: a review with emphasis on the projections of specific thalamic nuclei to the primary sensory areas of the neocotex." Brain Research Reviews **1**: 275-311.
Wilke, M., J. Turchi, K. Smith, M. Mishkin and D. A. Leopold (2010). "Pulvinar inactivation disrupts selection of movement plans." J Neurosci **30**(25): 8650-8659.
Wimmer, V. C., R. M. Bruno, C. P. de Kock, T. Kuner and B. Sakmann (2010). "Dimensions of a projection column and architecture of VPM and POm axons in rat vibrissal cortex." Cereb Cortex **20**(10): 2265-2276.
Wise, S. P. and E. G. Jones (1977). "Cells of Origin and Terminal Distribution of Descending Projections of the Rat Somatic Sensory Cortex." J Comp Neurol **175**: 129-158.
Xu, N. L., M. T. Harnett, S. R. Williams, D. Huber, D. H. O'Connor, K. Svoboda and J. C. Magee (2012). "Nonlinear dendritic integration of sensory and motor input during an active sensing task." Nature **492**(7428): 247-251.
Yamashita, T., A. Pala, L. Pedrido, Y. Kremer, E. Welker and C. C. Petersen (2013). "Membrane potential dynamics of neocortical projection neurons driving target-specific signals." Neuron **80**(6): 1477-1490.
Yassin, L., B. L. Benedetti, J. S. Jouhanneau, J. A. Wen, J. F. Poulet and A. L. Barth (2010). "An embedded subnetwork of highly active neurons in the neocortex." Neuron **68**(6): 1043-1050.
Zagha, E., A. E. Casale, R. N. Sachdev, M. J. McGinley and D. A. McCormick (2013). "Motor cortex feedback influences sensory processing by modulating network state." Neuron **79**(3): 567-578.
Zhou, M., F. Liang, X. R. Xiong, L. Li, H. Li, Z. Xiao, H. W. Tao and L. I. Zhang (2014). "Scaling down of balanced excitation and inhibition by active behavioral states in auditory cortex." Nat Neurosci **17**(6): 841-850.
Znamenskiy, P. and A. M. Zador (2013). "Corticostriatal neurons in auditory cortex drive decisions during auditory discrimination." Nature **497**(7450): 482-485.
Zucker, E. and W. I. Welker (1969). "Coding of Somatic Sensory Input by Vibrissae Neurons in the Rat Trigeminal Ganglion." Brain Research **12**: 138-156.

5.0 APPENDIX A: ESTIMATION OF RELATIVE LOCATIONS OF FUNCTIONAL SYNAPSES *IN VIVO*

5.1 INTRODUCTION

One of the most striking anatomical features of mammalian neurons is their tree-like elaborate and extensive dendritic arbor. Dendritic branches of central nervous system (CNS) neurons often extend hundreds of microns from the cell body, and are speckled with tens of thousands excitatory and inhibitory synapses. In addition to increasing the amount of surface area available for synaptic formation, dendrites also feature greatly in the way neurons integrate information they receive from other neurons. The electrotonic properties of the dendritic branches shape how synaptic current generated at a distant synaptic location affect the membrane potential of the neuron near its soma, where the action potential (AP) initiation zone is located. Decades of research have confirmed that dendritic filtering and integration of synaptic inputs are essential parts of neuronal information processing (Hausser and Mel 2003). For this reason, when investigating cortical neural circuitry and the neural computation, one might need to know not just how the neurons are connected to each other, but also the electronic filtering properties of their dendrites as well as the locations of the synapses on the dendritic tree.

Generally, to determine the subcellular anatomical distribution of different groups of synapses, one would employ 1) direct anatomical techniques: i.e. label presynaptic axons and postsynaptic neuron, and identify synaptic location by locating co-localization of pre-and postsynaptic markers under either confocal or electronic microscopy (Lu and Lin 1993, Feng, Kwon et al. 2014, Schoonover, Tapia et al. 2014); or 2) in-vitro optogenetic or electrical activation of the input neuronal populations while simultaneously imaging dendritic calcium activity in the postsynaptic neuron (for

example, ChR2-assisted circuit mapping, or sCRACM) (Petreanu, Mao et al. 2009). Both approaches require the use of either fixed brain tissue or living brain slices, and cannot be performed in the intact animal. It is therefore very difficult to obtain functional information (such as receptive fields) about the pre- or post-synaptic populations in the same study. Such information must be obtained through secondary studies.

In this chapter, we describe an attempt to devise a new method to probe relative dendritic locations of synapses *in vivo*. This method takes advantage of the passive filtering properties of dendrites themselves to probe locations of excitatory synapses activated by specific sensory stimuli. We also developed a realistic compartmental model of a single reconstructed cortical neuron to test and verify the validity of our method. However, the method is presently not workable due to the presence of feed forward inhibitory inputs elicited by the same sensory stimuli. Nonetheless, we believe that given an effective intracellular GABA antagonist reagent, one can use this method to probe synaptic locations on cortical neurons *in vivo*.

5.2 THEORETICAL BASIS OF THE IMPEDANCE METHOD

Dendrites are often modeled as an electrically leaky cable with a relatively low-resistance cytoplasm surrounded by a membrane consisting of resistive (ion channels) and capacitive (hydrophobic lipid bilayer membrane) elements in parallel (Rall 1962, Holmes and Rall 1992). The combination of these resistive and capacitive elements as well as the actual geometric shape of the dendritic branch will determine how the dendrites will filter and transmit electrical signals of various frequencies from the synapses to the soma – the impedance function of the dendrite. The impedance function of each neuron can be calculated by measuring the membrane voltage (V_m) while injecting the neurons with currents (I) of various frequencies. The impedance (Z) is then the resistance ($R = dV_m/dI$) for each frequency band.

While the impedance function of every dendritic tree is slightly different, they share a common general shape due to their shared physiological make-up: high frequency signals are much more filtered (low impedance) than low-frequency signals (higher impedance) (Rall 1962, Rall 1967, Rall, Burke et al. 1967, Smith, Wuerker et al. 1967, Rall and Rinzel 1973, Barrett and Crill 1974, Holmes and Rall 1992, Watanabe, Tsubokawa et al. 2014). This type of impedance function renders dendrites as low-pass filters for electrical signals (**Fig. 5.1A**). The direct consequence of this is that when a neuron is injected with a mixed frequency signal, the higher frequency signals will diminish fairly close to the site of injection while lower frequency signals can propagate farther down the dendritic tree (**Fig. 5.1B**).

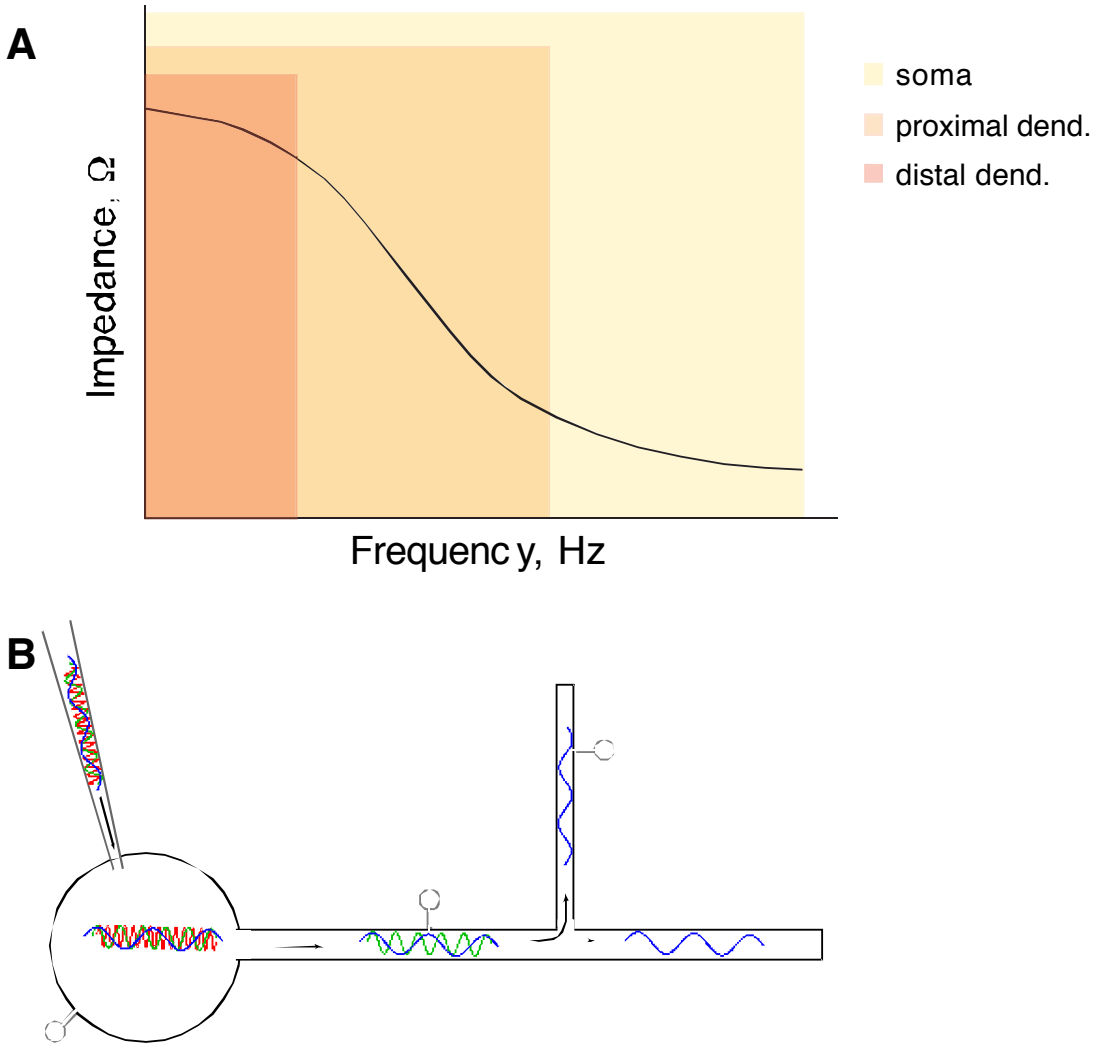

Fig 5.1 Impedance function of a neuron. (A) General shape of the impedance function of a neuron; (B) schematic of how a neuron filters mixed frequency current injections

The impedance function of the dendritic tree of a neuron is not static. In fact, it is constantly in flux. Synaptic transmission induces opening and closing of different ion channels, thus causing temporary changes in the filtering properties of the dendrites (Smith, Wuerker et al. 1967). In dendrites that contain voltage-gated ion channels (VGICs), modulations in the membrane potentials of the dendrites can also influence the impedance function of these dendrites. One can avoid engaging many of the VGICs of dendrites of mammalian CNS neurons by keeping the current injections used to probe the

impedance function low (typically <= ±300pA). Most VGICs are only significantly activated with large changes in Vm. One can also block VGICs pharmacologically to keep the dendrites completely electrically passive. We took a simplistic approach of assuming a passive dendritic tree and do not consider the contribution of VGICs.

Given that current injections of mixed frequencies will propagate down to different extents of the dendritic tree, synaptic events occurring at specific dendritic locations (proximal vs. distal) will have distinct influences on the impedance of the dendrite (Smith, Wuerker et al. 1967). Regardless of synaptic strength, synapses located on the proximal dendritic branches would affect the V_m responses to both high and low frequency currents; whereas synapses located on the more distal part of the dendritic tree would only experience low frequency currents, and therefore only influence the V_m responses in the low frequency band (Maltenfort, Phillips et al. 2004). Therefore, if we measure the impedance function of the neurons during different periods of synaptic transmission, one can, in theory, determine the relative locations of the synapses based on how the impedance function changed in real time. This method has been tested and demonstrated to be feasible in locating Renshaw recurrent inhibition in spinal motoneurons of cats, and serves as our inspiration for this project (Maltenfort, McCurdy et al. 2004).

Given this method, one can effectively probe relative synaptic locations *in vivo* in real time. The synapses being compared don't have to be organized anatomically (i.e. by different presynaptic areas), but can be organized functionally (i.e. engaged by different sensory inputs). In our experiments, we attempt to test the hypothesis that in barrel

cortex L4 neurons, synapses mediating the preferred direction of whisker deflection are located more proximally than synapses mediating the non-preferred direction.

5.3 EXPERIMENTAL DESIGN AND RESULTS

Experiments were performed in urethane-anesthetized female Wistar rats (150-250g).

Version 1.0

In each experiment, we perform whole-cell patch clamp recording from L4 barrel neurons. Once a reasonable patch-clamp recording is established, we inject the neuron with DC currents of different amplitudes (-300pA to 400pA in 50-100pA intervals) and measure the voltage responses of the neuron. We then calculate the current-voltage response (I-V) curve of the neuron online. Since nonlinearity in the I-V curve is indicative of involvements of VGICs, we need to determine the voltage range within which the I-V curve of the neuron remains relatively linear. Once we find the linear voltage range and the amplitude of the current needed to induce it, we can then obtain the resting impedance function of the neuron by inject a frozen pink noise ($\leq$ 200Hz) current with maximum amplitude that is within the linear range of the cell into the neuron.

Once we complete probing the basic electrotonic properties of the neuron, we then map the receptive field by measuring the neuron's subthreshold responses to deflections of the PW of the neuron randomly in each of eight directions, in 45° increments relative to the horizontal alignment of the rows. Whiskers were positioned inside the stimulator ~10 mm from the base of the hair and deflected 5.7° (1-mm amplitude) using relatively high-velocity (onset and offset: ~570° / sec) ramp-and-hold movements. A receptive field was mapped by applying 10-20 blocks of these stimuli (80-

160 total stimuli with 2-second interstimulus intervals). We then apply deflections in the preferred and least preferred directions in randomly interleaved trials while injecting the neuron with the same frozen pink-noise previously used to measure how sensory inputs modify the impedance function of the neuron (**Fig. 5.2**). Since we need prolonged synaptic activation by whisker stimuli so that the synapses are activated over the duration of the pink-noise, we used a slow, relatively weak periodic whisker stimulus instead of the fast ramp-and-hold stimuli for this part of the experiment.

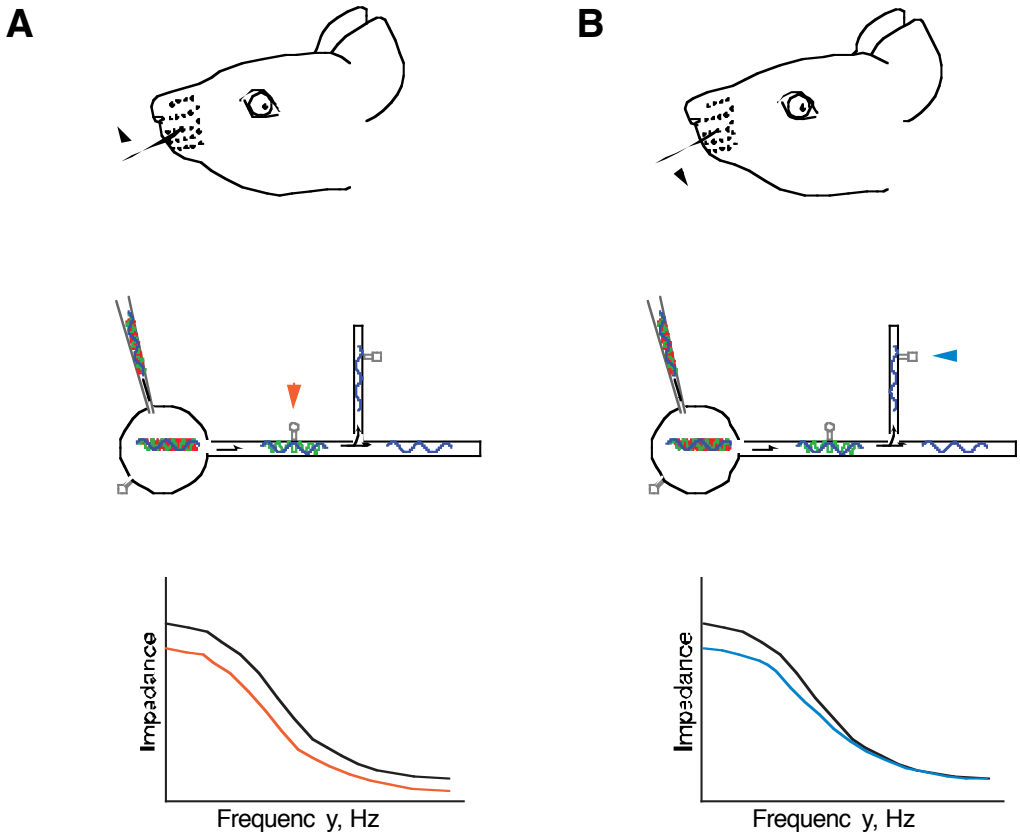

Fig 5.2 Experimental setup version1. (A) Top: stimulation of PW in the preferred direction; Middle: injection of pink noise current and while sensory input induces synaptic current in the proximal synapse (red arrow); Bottom: predicted impedance change during preferred stimuli (red) vs. baseline impedance of the neuron (black); (B) Top: stimulation of PW in the least-preferred direction; Middle: injection of pink noise current and while sensory input induces synaptic

current in the distal synapse (blue arrow); Bottom: predicted impedance change during preferred stimuli (blue) vs. baseline impedance of the neuron (black)

By obtaining the impedance functions of the neuron under different conditions, we can compare if synapses engaged by the preferred and least preferred directions of whisker deflection differentially modified the dendritic impedance properties of the neuron. If our initial hypothesis (synapses representing the preferred whisker stimulus are located more proximally to the soma than the least-preferred stimulus) was correct, the impedance (Z) measured during PW deflection in the preferred direction should decrease over most if not all frequencies; whereas Z measured during PW deflection in the least preferred direction should decrease only in the low frequency band (**Fig. 5.2**, bottom). In **Fig. 5.3** is an example neuron. The preferred direction (**Fig. 5.3A**) has the most decrease in impedance in the broadest band of frequencies while the least preferred direction has the least decrease in impedance in only the lowest frequencies (**Fig. 5.3B**). However, most of our neurons recorded did not behave this way, and our results proved ambiguous.

During our experiments, we discovered several factors that made this particular version of the experimental design difficult to achieve:

1) The whole protocol requires patching the neuron for up to an hour while the recording quality remains relatively unchanged. This is very difficult to achieve *in vivo*. Even when we can hold the recording for up to an hour, very often the quality of the recording would deteriorate near the end of the session. The change in recording quality itself changes the filtering properties we measure during the experiment, and would introduce unknown amount of variable noise to our experiments.

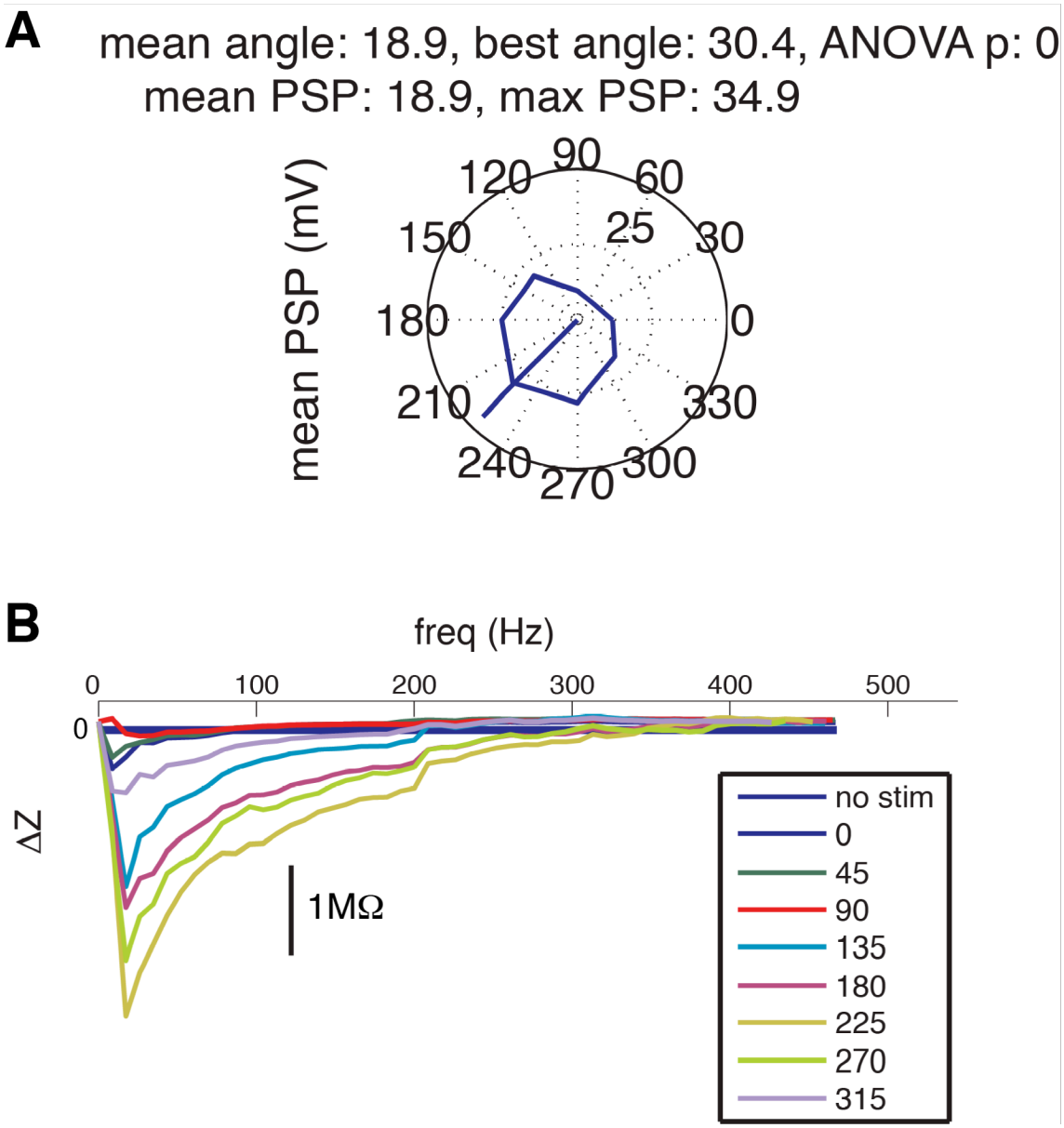

Fig 5.3 Example impedance analysis data. (A) Polar plot of the recorded neuron (B) Impedance change of the neuron during different PW stimulation directions.

2) To get data about Z in the low frequency bands, we must maintain synaptic activation for long periods of time, which is why we decided to use the slow, periodic whisker stimuli. However, because we must use the entire trial length worth of data, background synaptic events can introduce significant amount of

noise. Moreover, by definition, during half of the periodic stimulus the whisker is deflected in the opposite direction of the preferred direction, which is very often the least preferred direction.

For these reasons, the data we collected using this set of protocols proved to be noisy and difficult to interpret. However, we were able to generate a full 3D reconstruction of one barrel-related spiny stellate neuron, and use the anatomical and physiological data we collected to create a NEURON model of the cell. We simulated how current of different frequencies injected at the soma of this neuron would dissipate at it propagate down the dendrites. The model demonstrated that in the case of a typical L4 neuron recorded *in vivo* under urethane anesthesia, even DC current injections dissipate significantly by the time it reaches the proximal dendrites (**Fig. 5.4**). Given this finding, as well as the previously mentioned technical difficulties involved with the existing experimental protocol, we decided to revise and simplify the design of the experiment.

Version 2.0

The new experimental protocol took advantage of the fact that DC current injection at the soma dissipates quickly in L4 dendrites. By this logic, currents injected at the soma will modulate the local V_m at proximal dendrites more than local V_m at the distal dendrites. Furthermore, driving force for synaptic currents located at the proximal segments of the dendrites will be more affected by this current injection than distal synapses. So, instead of using pink noise current, we injected the neurons with various levels of DC current (-200 pA to +300 pA, in 100pA steps) while deflecting the PW in

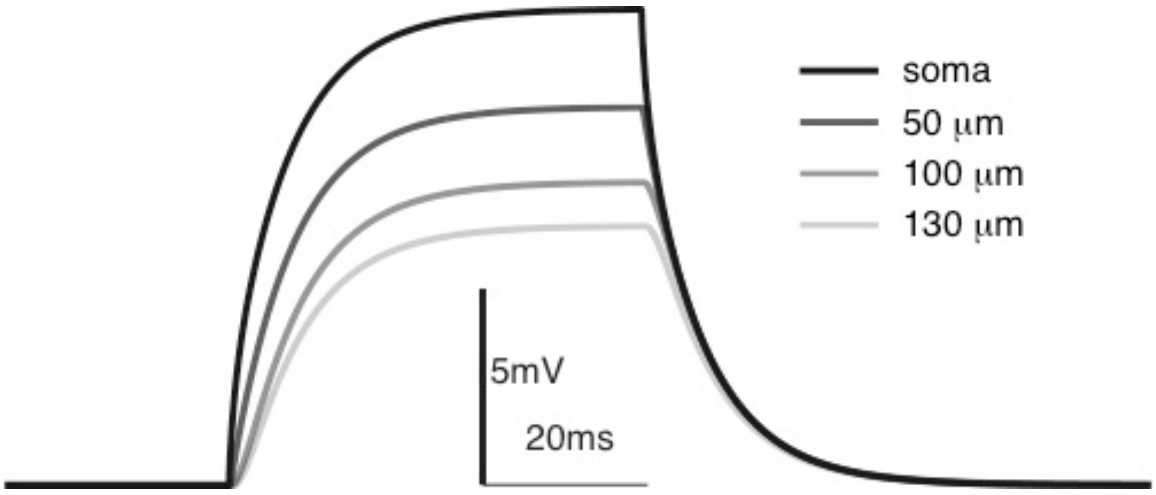

Fig 5.4 Attenuation of DC current in L4 model neuron. In the reconstructed L4 neuron, we simulated a 100pA current injection at the soma, and recorded the voltage response at the soma, and dendritic locations 50, 100, and 130mms away from the soma.

the preferred and least-preferred directions (**Fig. 5.5A**). We then measure the peak of the EPSPs elicited by the whisker deflection at different current levels. Since the proximal synapses would experience more V_m modulations than distal synapses, if we plot V_{peak} vs. current level (I), the proximal synapses (preferred direction) should have a much steeper V_{peak}/I relationship than distal synapses (least-preferred direction) (**Fig. 5.5B**). The advantage of this approach is that the analysis is fairly simple and straightforward. Also since we are only concerned with measuring the peak PSP, we can use the ramp-and-hold stimulus and limit our analysis to the on-responses of the neuron.

Our results from this new protocol proved to be inconclusive. The V_{peak}/I slopes we measured were variable and didn't show any predictable trends. Given this data, I hypothesized that feed forward inhibition from local inhibitory neurons maybe causing the ambiguity. I tested the hypothesis with my existing NEURON model by inserting a random set of inhibitory synapses that are spaced uniformly in the dendritic tree. We then inserted two separate populations of excitatory synapses, one within 100ums of the soma

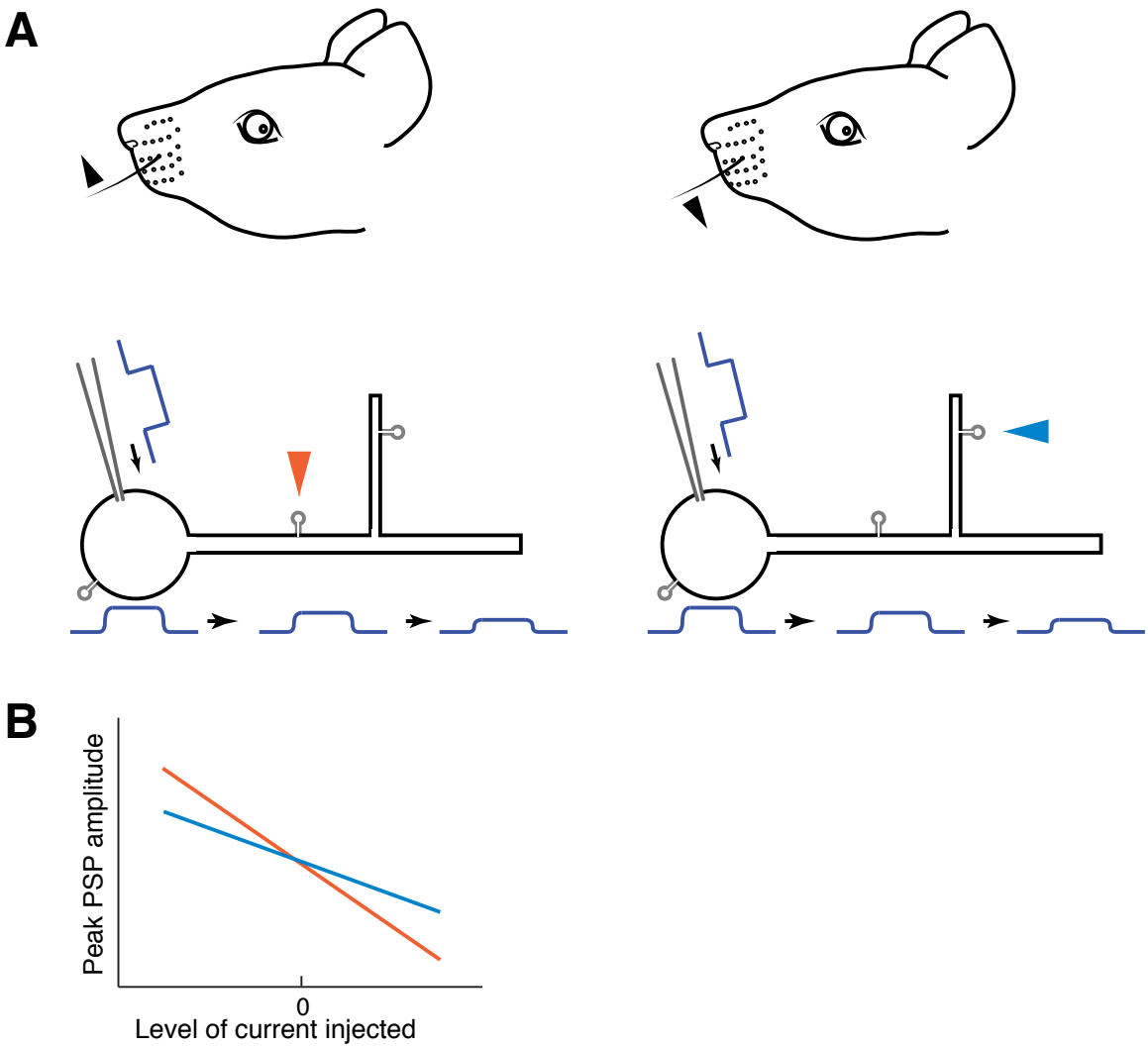

Fig 5.5 Experimental setup version 2. (A) Left: PW stimulation in the preferred direction (activating proximal synapses, red arrow) while injecting different levels of DC current; Right: PW stimulation in the least-preferred direction (activating distal synapses, blue arrow) while injecting different levels of DC current. (B) Predicted V-I plots for proximal (red) vs. distal (blue) synaptic activation.

(proximal), and the other at least 100ums away (distal). Once the model neuron is properly set up, we can simulate the experimental situation with our model. I injected DC currents of different amplitudes into the soma of the model neuron while activating either

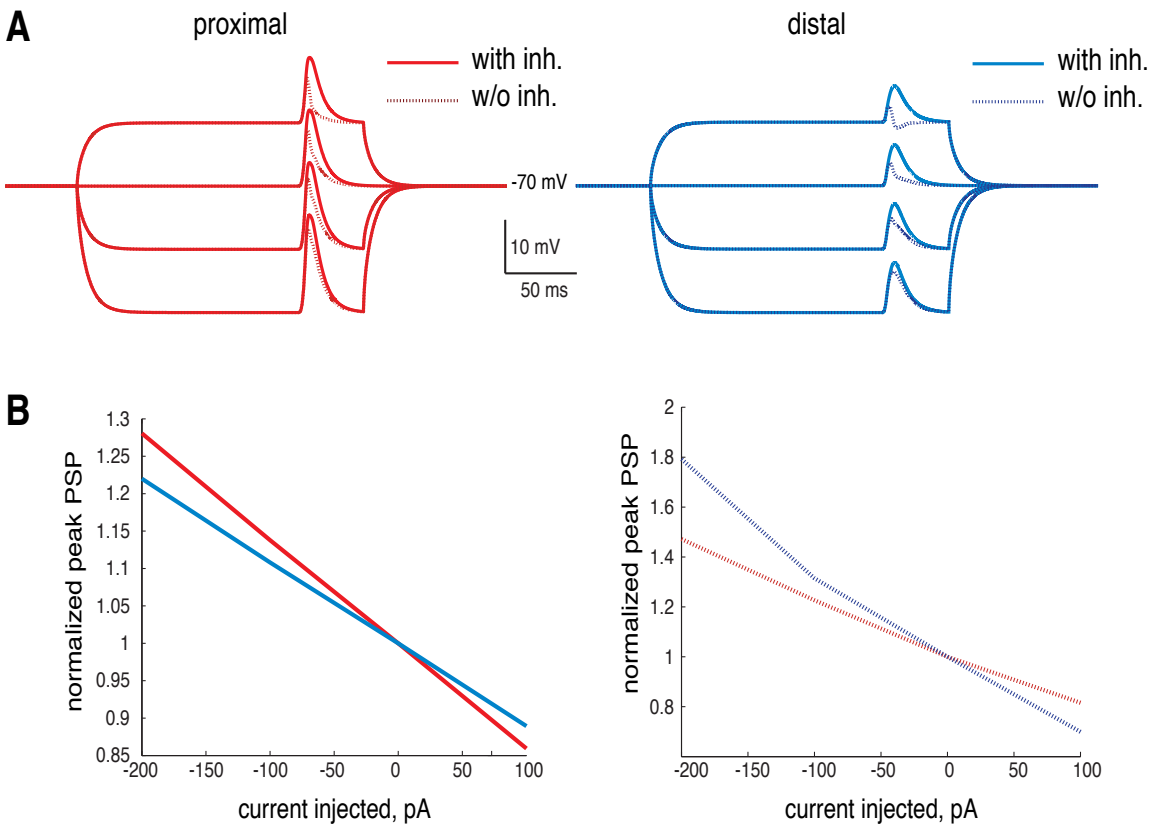

Fig 5.6 NEURON simulation of the DC attenuation method. All recordings are done at the soma. (A) Simulation of activation of proximal (left, red) and distal (right, blue) excitatory synapses while injecting +100, -100, and -200pA DC current at the soma, with (dotted line) and without (solid line) feed forward inhibition; (B) V-I plot of peak PSP amplitude measured at the soma for proximal (red) vs. distal (blue) excitatory synapses, with (right) and without (left) feed forward inhibition.

the proximal or distal excitatory synapses. In some cases we also activated all the inhibitory synapses simultaneous with the excitatory synapses (**Fig. 5.6A**). We measure the V_m responses to these synaptic activities at the soma, and repeated our analysis for the data we collected from the model neuron. The model confirmed our suspicion: without feed forward inhibition, our method works well as a way to detect relative synaptic location, however, when we included feed forward inhibition that are randomly

distributed, the slope of the V_{peak}/I curve can no longer accurately predict the relative location of the excitatory synapses (**Fig. 5.6B**).

To solve this issue, we tried repeating the electrophysiology experiments while pharmacologically blocking the inhibitory synaptic currents (GABAa) within the neurons from which we were recording. This venture proved fruitless as all of the GABA antagonists that have been published to date failed to work intracellularly, even at unusually high concentrations:

TS-TM (1μM – 1mM) (Dudek and Friedlander 1996)

DNDS (0.5mM – 5mM) (Nelson, Toth et al. 1994, Dudek and Friedlander 1996)

Picrotoxin (25μM – 1mM) (Inomata, Ishihara et al. 1988)

Given this result, we finally decided that it is not feasible to intracellularly block inhibitory synapses given the current technology. Therefore we decided to not pursue this project any further.

5.4 ALTERNATIVE APPROACH

Recently Kawashima, et. al. published a new method using a synthetic activity-dependent promoter enhanced synaptic activity-responsive element (E-SARE) to functionally label neurons as well as their axons *in vivo* (Kawashima, Kitamura et al. 2013). The E-SARE reporter system preferentially marked neurons that showed high sensory-driven firing over neurons with high spontaneous firing rate. Moreover, the synthetic promoter drives neuronal activity-dependent gene expression more potently than other existing immediate-early gene promoters. An AAV-expresssing E-SARE-driven dGFP virus has been used to successfully label thalamocortical axons from LGN to mouse V1. Given this new tool, I propose a new anatomical method to approach this project.

Experimental Design:

To limit the E-SARE driven expression in response to only specific sensory stimuli, we can inject one barrelloid of the rat VPM with E-SARE-driven $ER^{T2}CreER^{T2}$ expressing virus as well as a virus encoding Cre-dependent synaptohysin-eGFP expression. We then juxtasomally record and fill a L4 excitatory neuron in the aligned barrel. After mapping the preferred direction of deflection of said L4 neuron, we then subject the rat to a 6-hr stimulation paradigm of the PW in the preferred direction along with tamoxifen administration immediately before whisker stimulation. The whisker stimulation paradigm should be designed so that the on-phase of the stimulation (the phase that is a deflection in the preferred direction) should be fast, while the off-phase

(deflection to the opposite direction to return the whisker to resting position) should be as slow as possible so that we are maximally activating thalamic neurons share the preferred direction as the recorded cortical neuron.

We would then perfuse the animal and retrieve the brain. We would anatomically identify the synapses formed on the filled cortical neuron by the synaptophysin-eGFP-positive thalamocortical axons. If our hypothesis is correct, we should be able to observe that the synaptophysin-eGFP-positive boutons preferentially form synapses on the proximal dendritic branches of L4 neurons. If the spatial distribution of the synapses is random, then our hypothesis would be proven incorrect.

5.5 CONCLUDING REMARKS

While it is always disappointing when a carefully planned project fails to pan out, I believe this is one of the most rewarding experiences I have had during my graduate career. Not only did it allow me to learn a whole list of skills (in electrophysiology, immunohistochemistry, as well as using NEURON as a modeling language), but also let me gain extremely valuable experiences in designing, updating and refining experimental protocols. In retrospect, it would have been useful to test the method of using impedance analysis to predict relative synaptic locations prior to using it on a untested hypothesis. Perhaps the process would have been less frustrating had we tested and refined the method on groups of known proximal vs. distal synapses *in vivo* under otherwise similar experimental conditions (for example, PW stimulation elicited synapses vs. AW stimulation elicited synapses). It was at times infuriating when I was not able to determine whether my ambiguous result was indicative of the method failing or confirmation of the null hypothesis. It was ultimately rewarding to know that the project failed due to technical issues as opposed to conceptual limitations, and it is even more satisfying to be able to propose a promising alternative approach to investigate the problem 5 years later.